

PARTICLE IDENTIFICATIONS IN SIDIS RECONSTRUCTIONS

SIDIS PWG meeting for ePIC

June 11° 2024

Lorenzo Polizzi | University of Bologna

DATA ANALYZED

This analysis presents the production of positive and negative **pions**, **kaons** and **protons** as a function of different kinematic variables over their kinematic range with PDG code PID performance.

The data are taken from (event analyzed from 1885 to 1888):

[dtn-eic.jlab.org//work/eic2/EPIC/RECO/24.05.0/epic_craterlake/
SIDIS/pythia6eic/1.0.0/18x275/q2_0to1](https://dtn-eic.jlab.org//work/eic2/EPIC/RECO/24.05.0/epic_craterlake/SIDIS/pythia6eic/1.0.0/18x275/q2_0to1)

[pythia_ep_noradcor_18x275_q2_0.000000001_1.0_run9.ab.1885-1888.eicrecon.tree.edm4eic.root](#)

VARIABLE RECONSTRUCTION

The variables of interest are Q^2 , x_B , z , P_{hT} , η , φ (polar angle) and the momentum.

The DIS variables are reconstructed with the Double Angle method:

$$y = \frac{\tan \frac{\varphi}{2}}{\tan \frac{\varphi}{2} + \tan \frac{\theta}{2}} \quad Q^2 = 4E_0^2 \cot \frac{\theta}{2} (1 - y) \quad x_B = \frac{Q^2}{4E_0 E_p y}$$

Where y is the inelasticity, θ represents the polar angle of the scattered electron and E_0 and E_p are the respective energy of the electron and proton beam.

VARIABLE RECONSTRUCTION

The SIDIS variables follow the theory and are defined as:

$$z = \frac{P \cdot P_h}{P \cdot q} \quad \vec{P}_{hT} = \vec{P}_h - \frac{\vec{P}_h \cdot \vec{q}}{|\vec{q}|} \hat{q}$$

P denotes the momentum of the target hadron, P_h represents the momentum of the identified hadron, and q is the momentum of the virtual photon.

The regions with positive rapidity are the one along the proton beam direction, consequently, the electron beam direction refers to negative rapidity values.

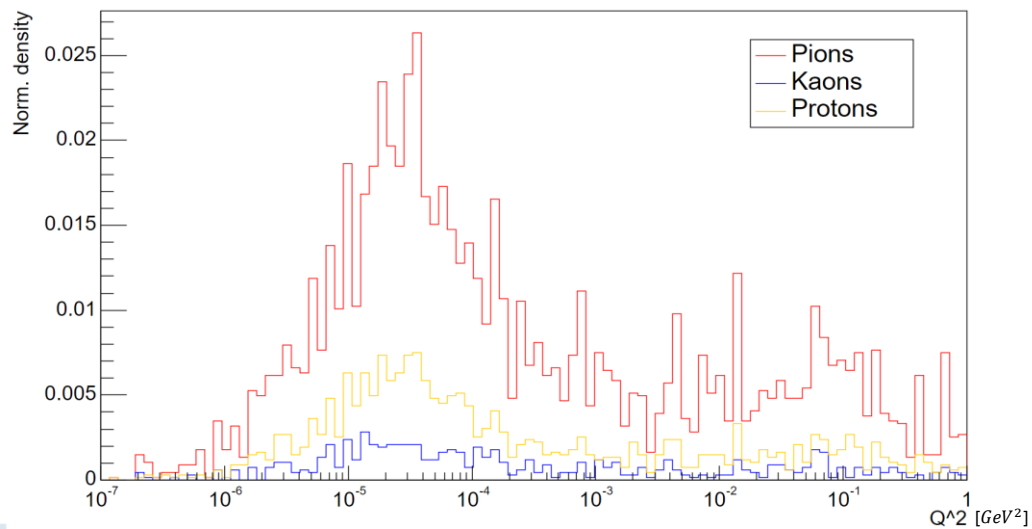
PLOTS

Three type of plots are displayed in the next slides:

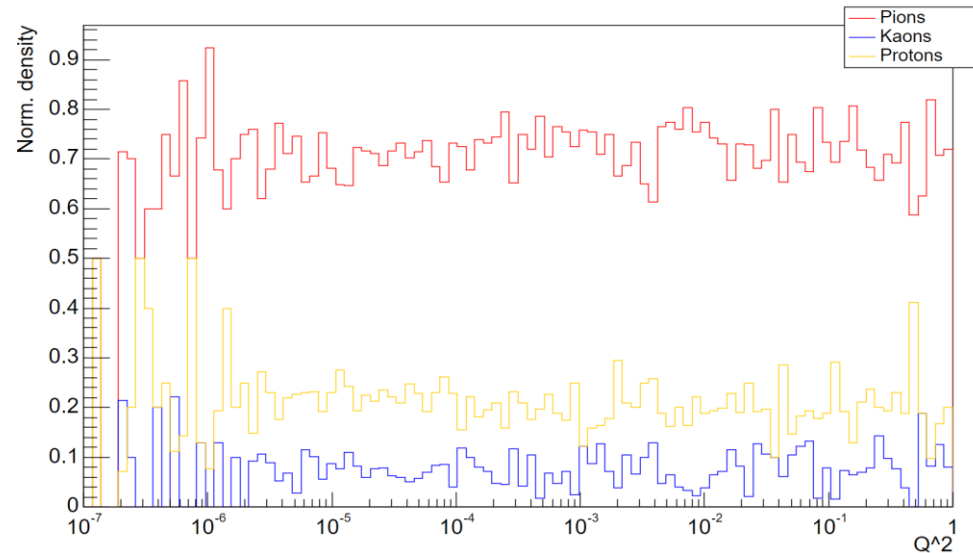
1. Particle production normalized over the summed area of the three histograms to show their densities in different kinematic regions.
2. Relative fraction of particle types normalized over the sum of each bin content.
3. Reconstruction efficiency of the three hadron types, calculated as the fraction of reconstructed data over the MC generated data.

NORM. COUNTS vs Q^2 | POSITIVE CASE

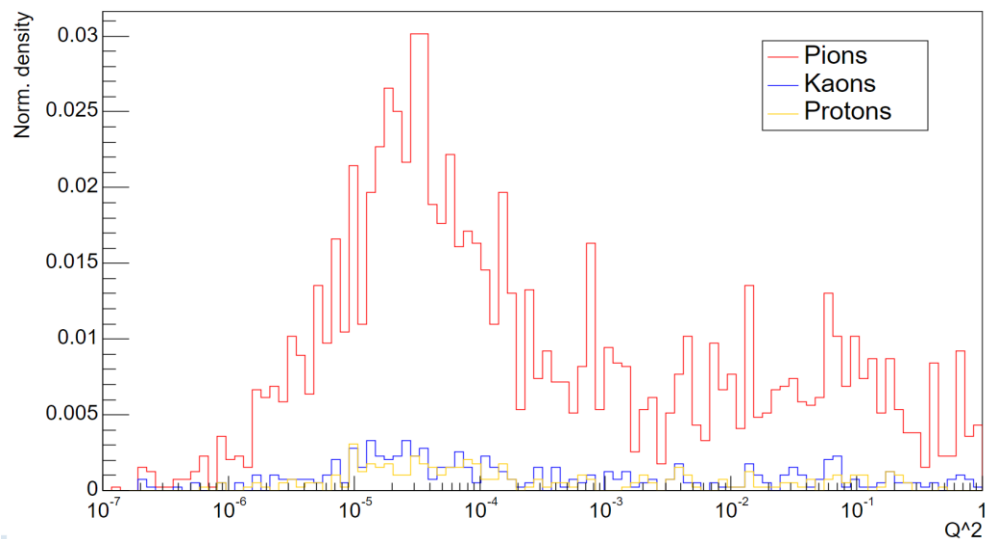
MC Production of positive particles | 18x275 GeV



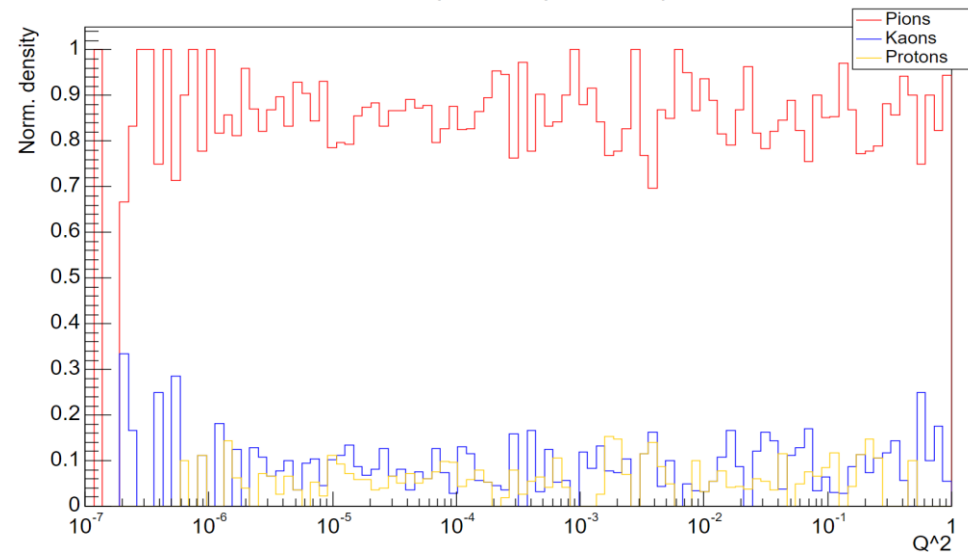
MC Production of positive particles | 18x275 GeV



Reconstruction of positive particles | 18x275 GeV

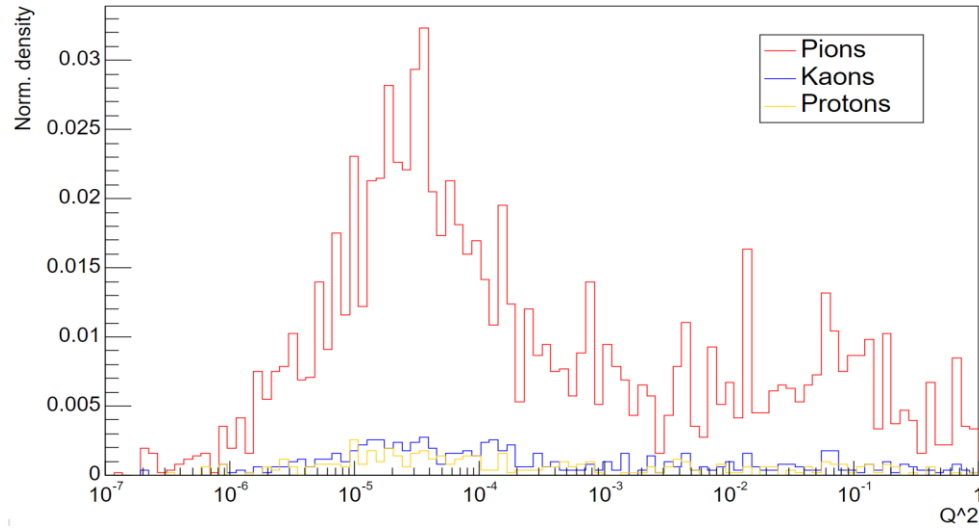


Reconstruction of positive particles | 18x275 GeV

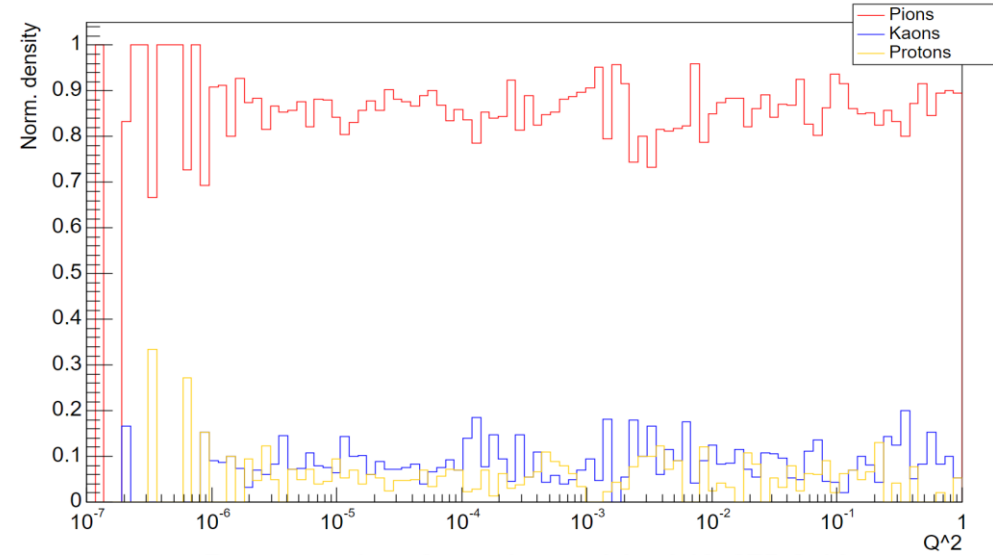


NORM. COUNTS vs Q^2 | NEGATIVE CASE

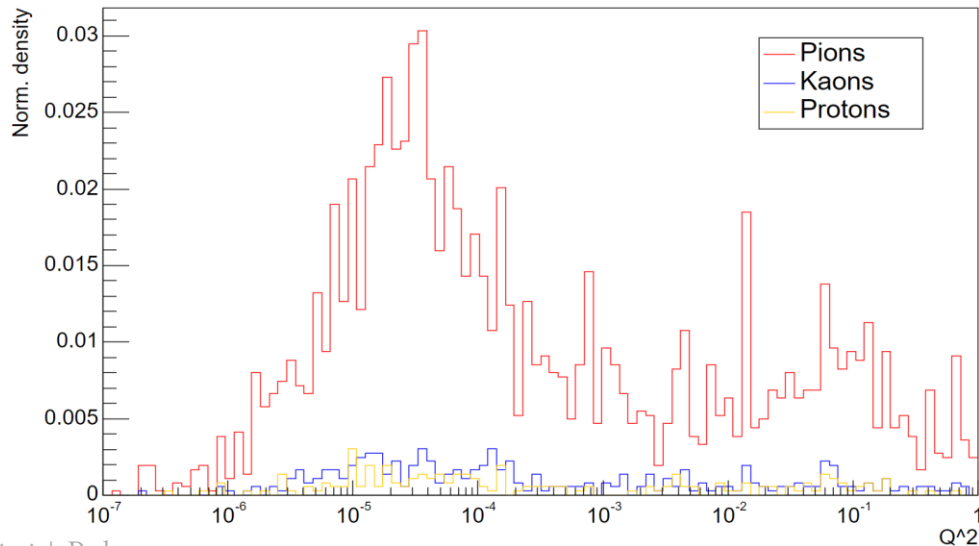
MC Production of negative particles | 18x275 GeV



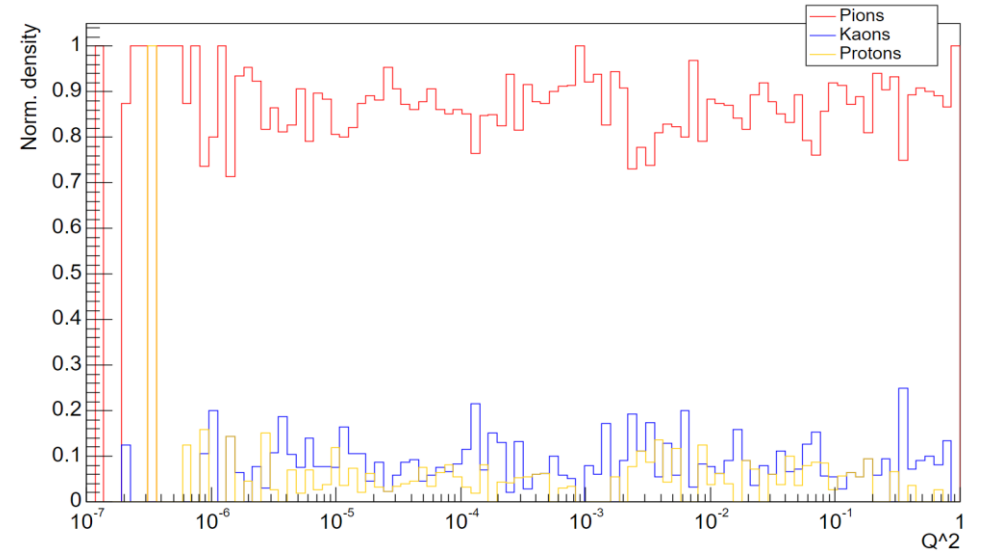
MC Production of negative particles | 18x275 GeV



Reconstruction of negative particles | 18x275 GeV

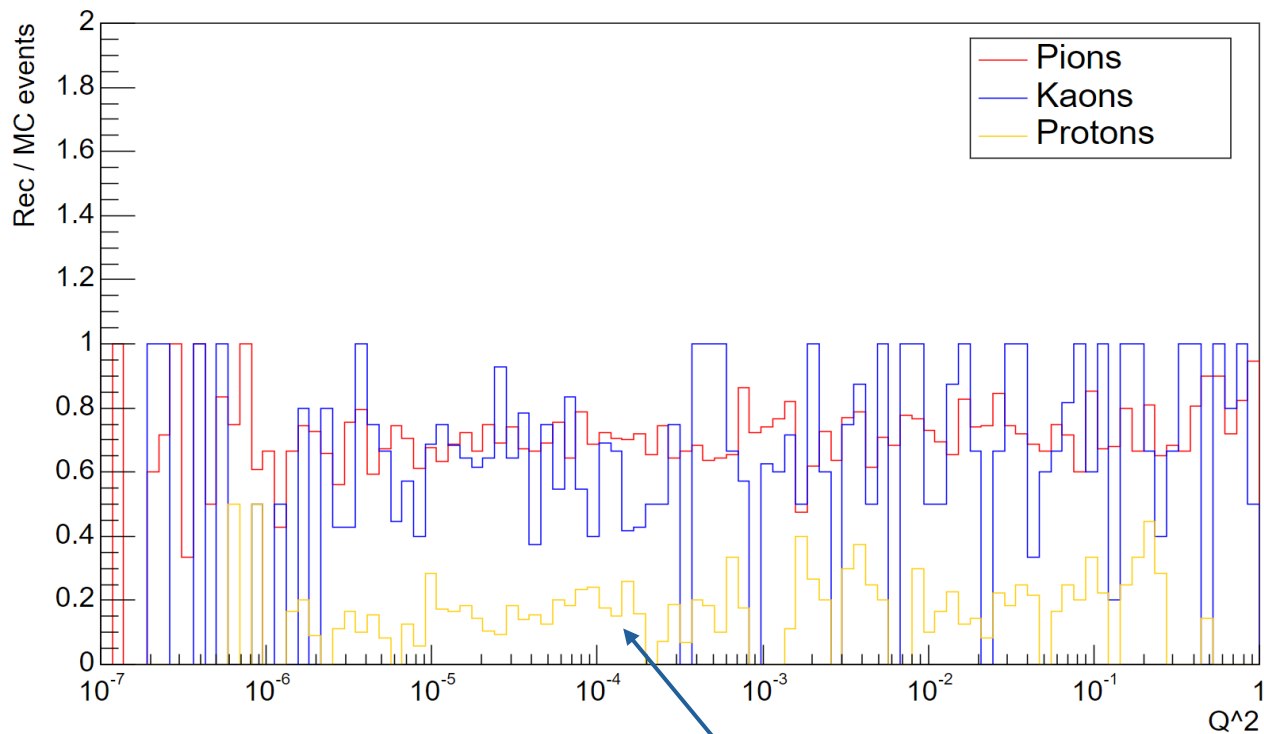


Reconstruction of negative particles | 18x275 GeV



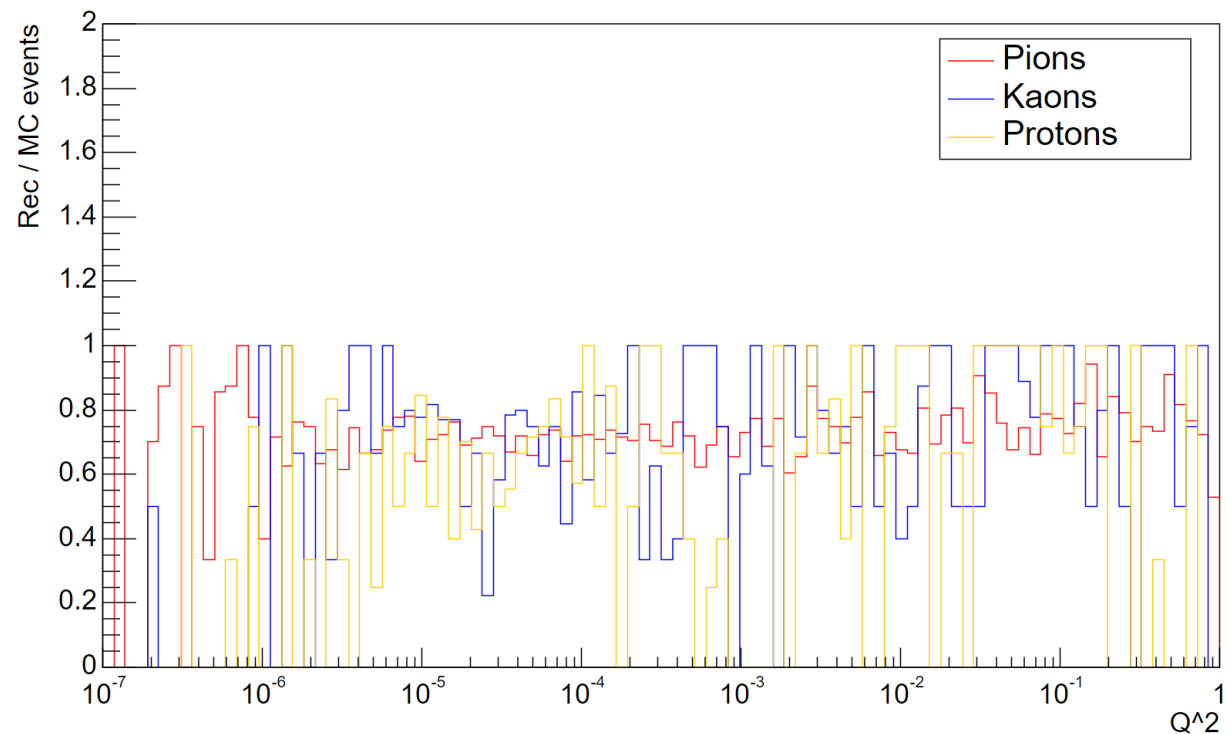
EFFICIENCY VS Q^2

Efficiency reconstruction of positive particles | 18x275 GeV



Low efficiency in the proton reconstruction

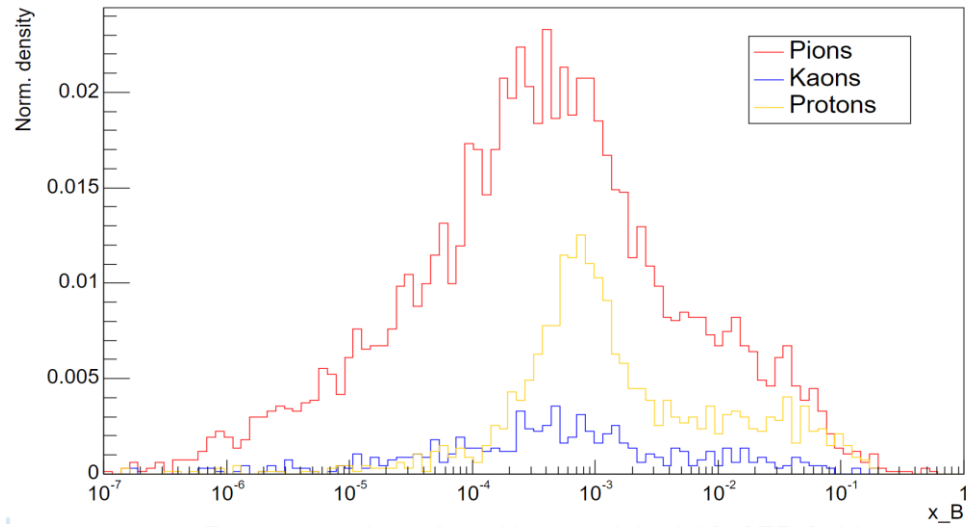
Efficiency reconstruction of negative particles | 18x275 GeV



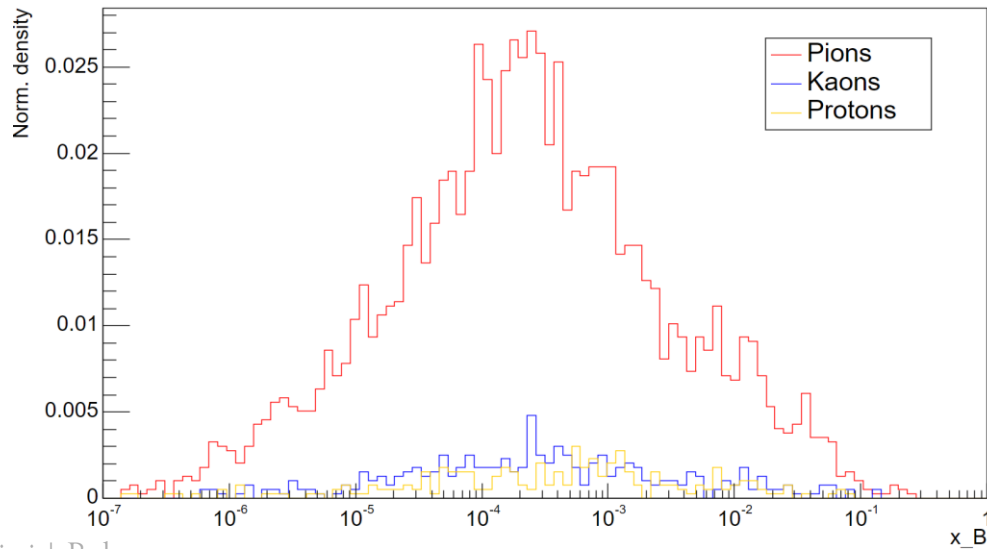
NORM. COUNTS vs x_B

POSITIVE CASE

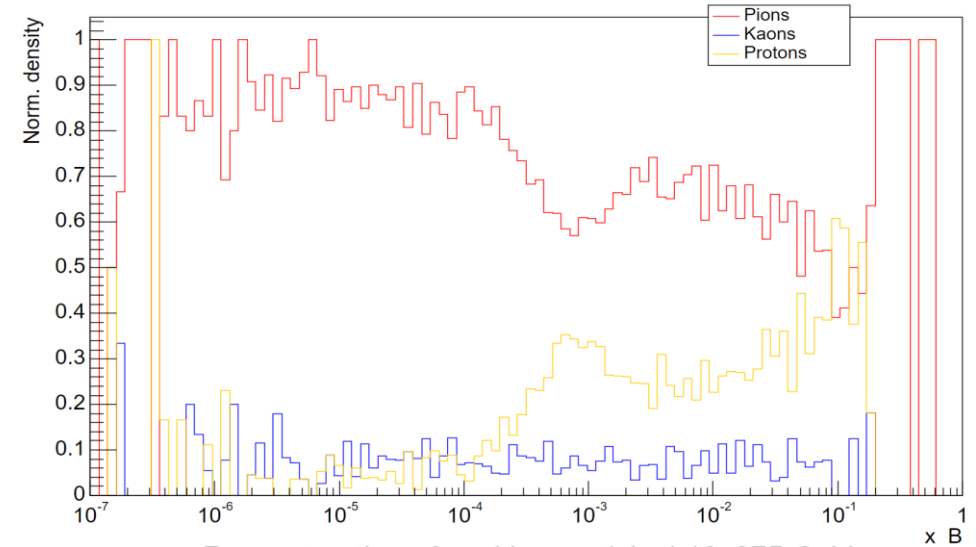
MC Production of positive particles | 18x275 GeV



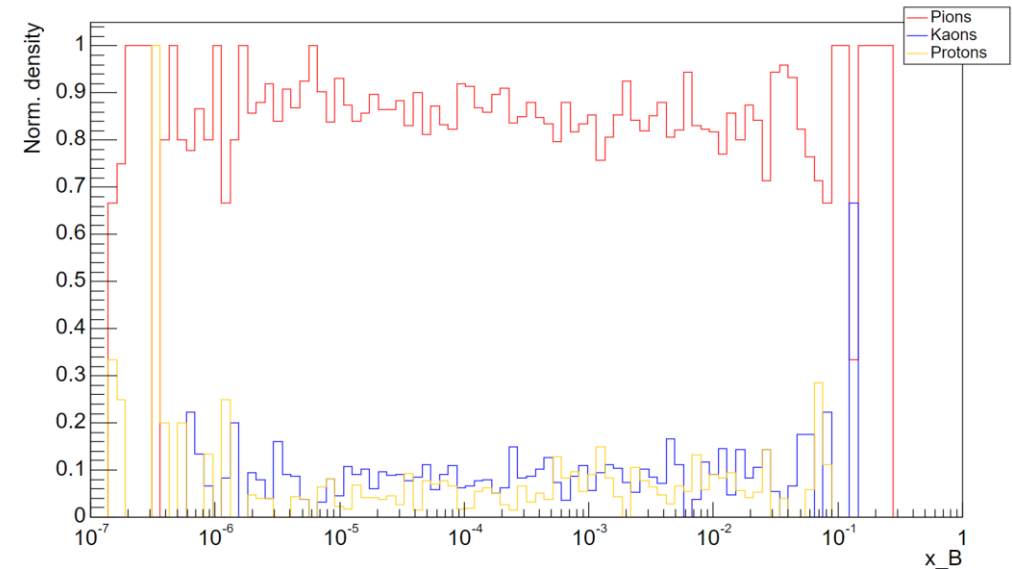
Reconstruction of positive particles | 18x275 GeV



MC Production of positive particles | 18x275 GeV

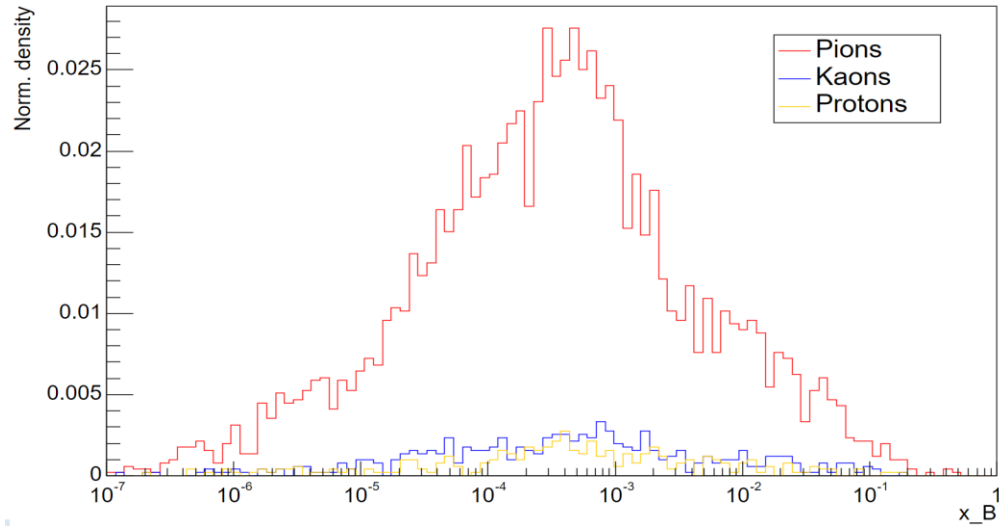


Reconstruction of positive particles | 18x275 GeV

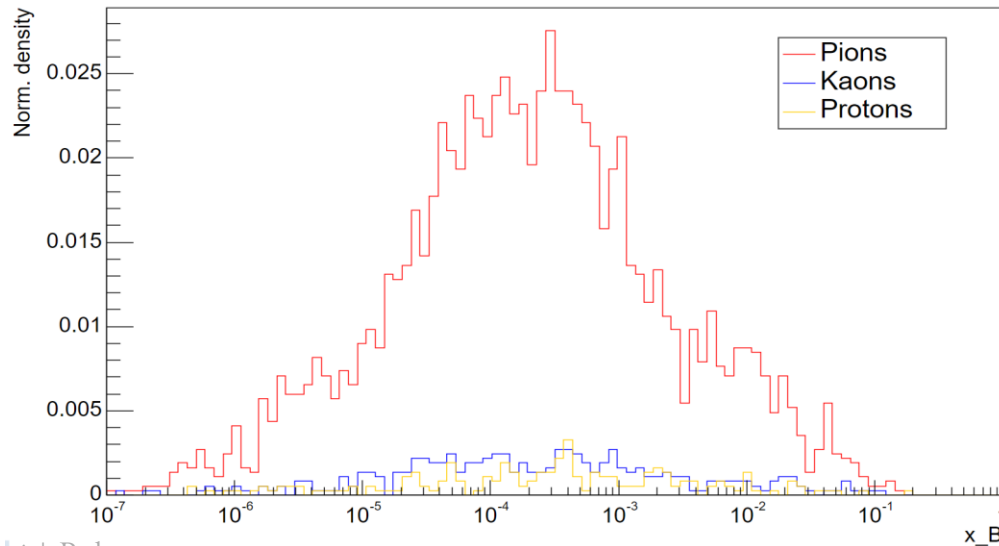


NORM. COUNTS vs x_B | NEGATIVE CASE

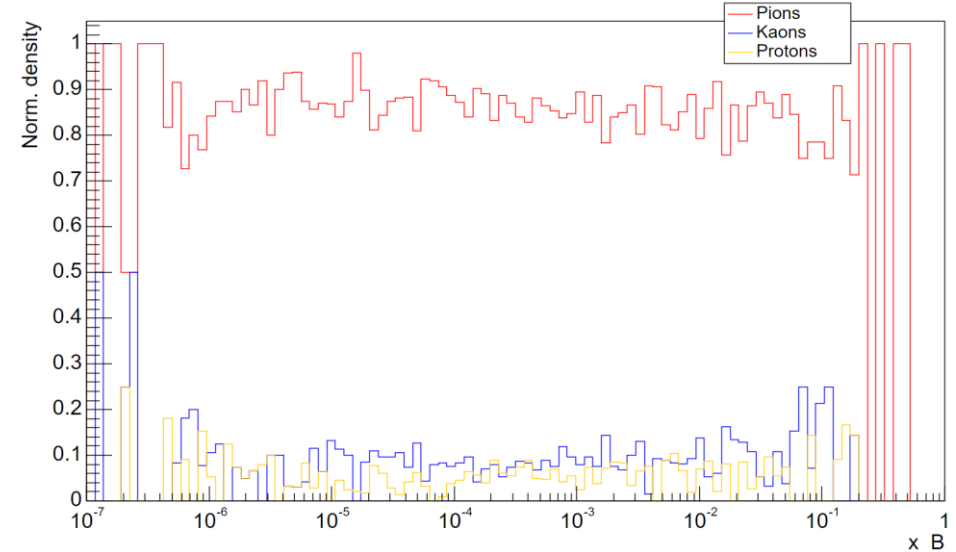
MC Production of negative particles | 18x275 GeV



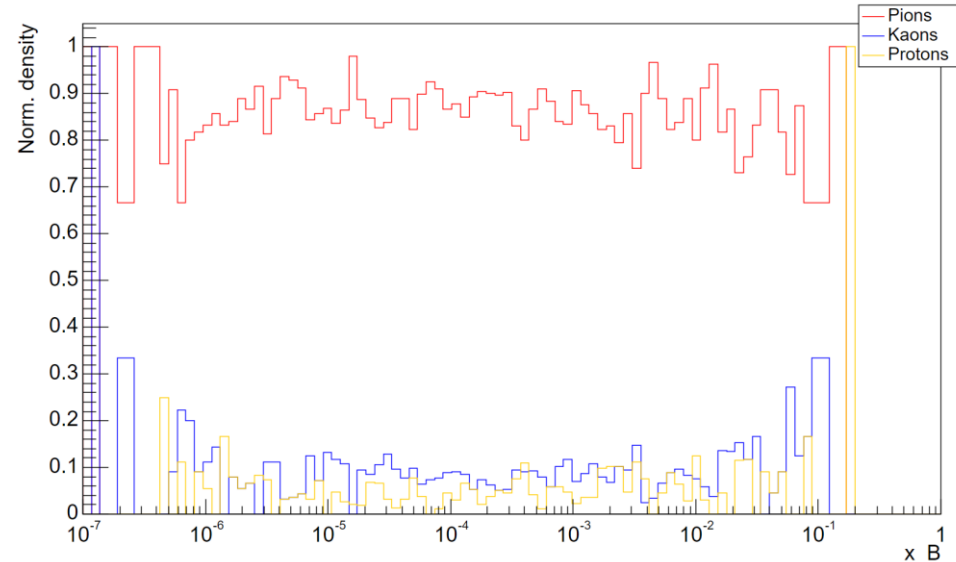
Reconstruction of negative particles | 18x275 GeV



MC Production of negative particles | 18x275 GeV

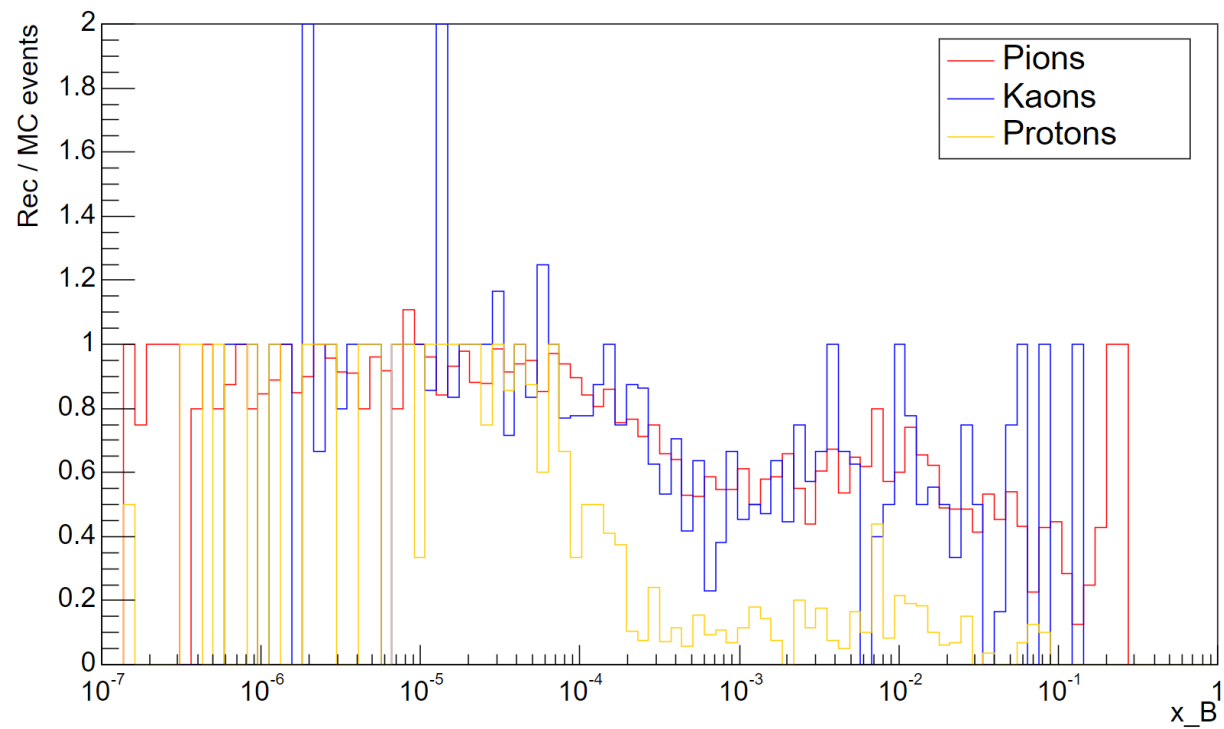


Reconstruction of negative particles | 18x275 GeV

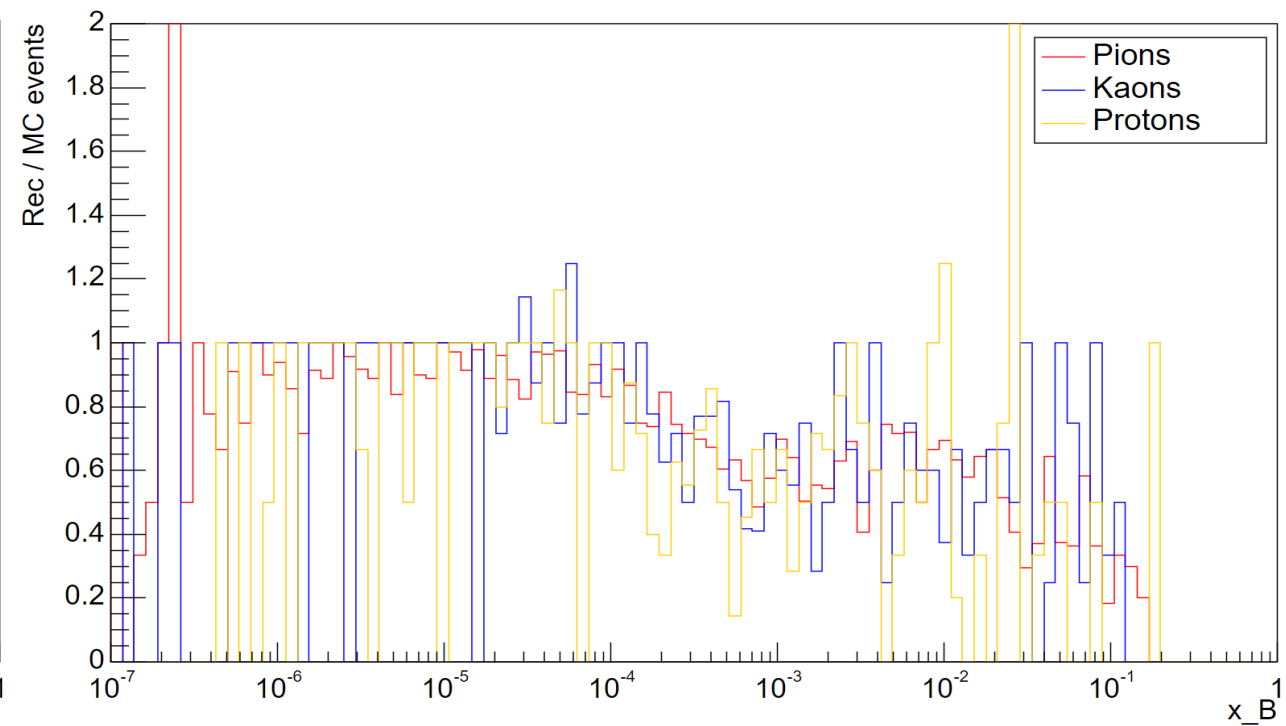


EFFICIENCY VS x_B

Efficiency reconstruction of positive particles | 18x275 GeV

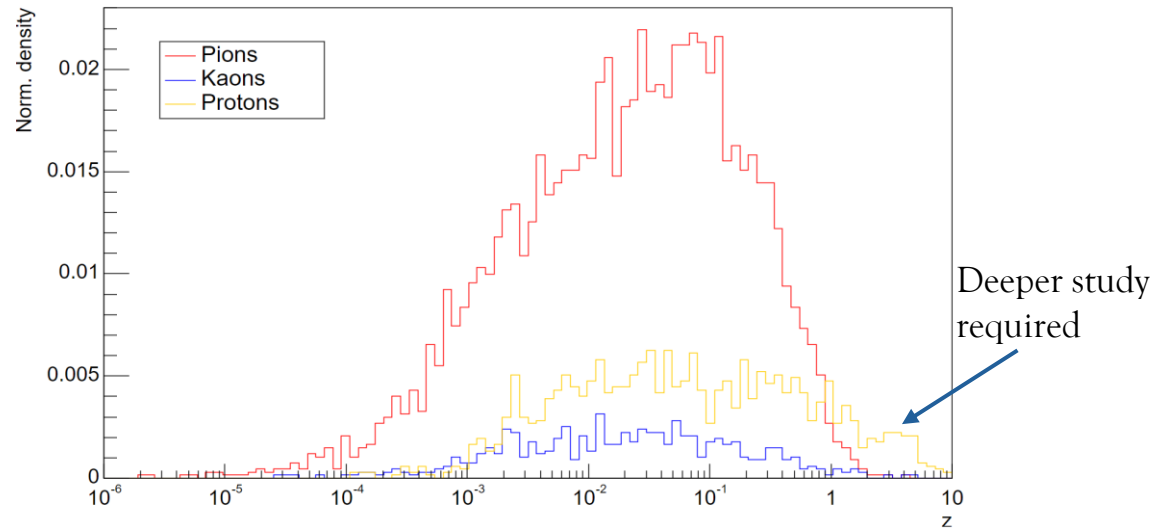


Efficiency reconstruction of negative particles | 18x275 GeV

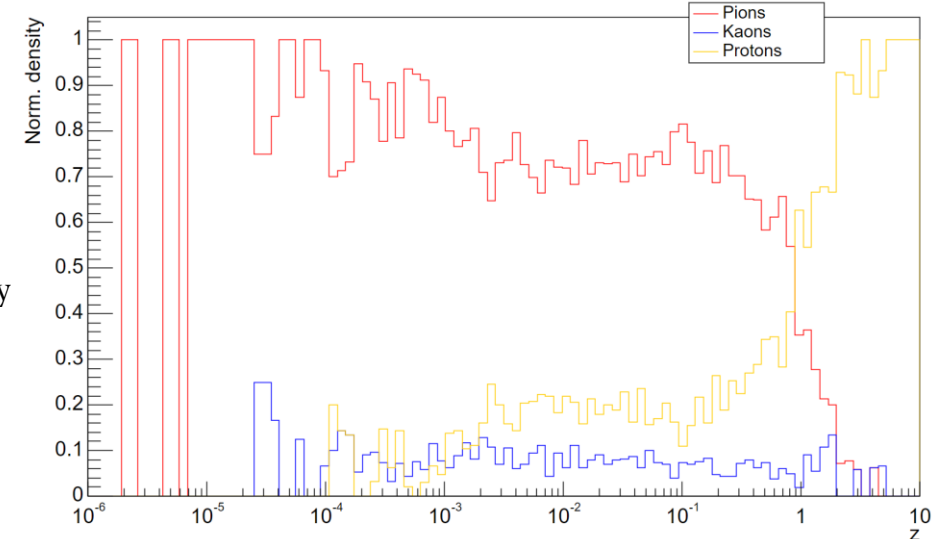


NORM. COUNTS vs z | POSITIVE CASE

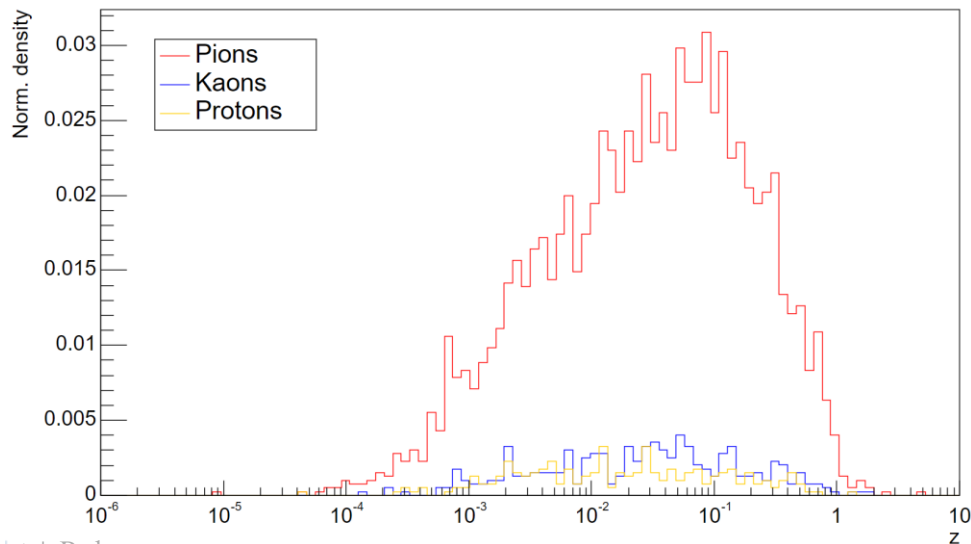
MC Production of positive particles | 18x275 GeV



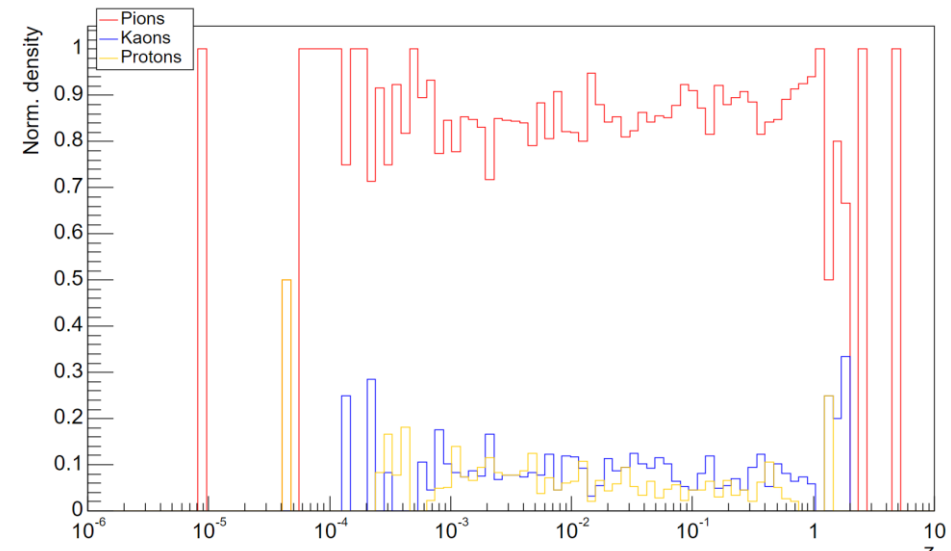
MC Production of positive particles | 18x275 GeV



Reconstruction of positive particles | 18x275 GeV

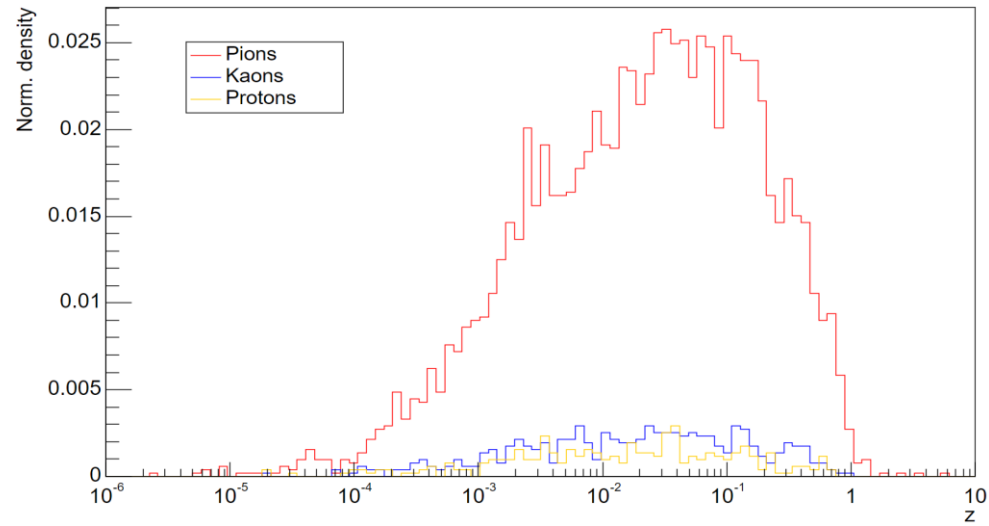


Reconstruction of positive particles | 18x275 GeV

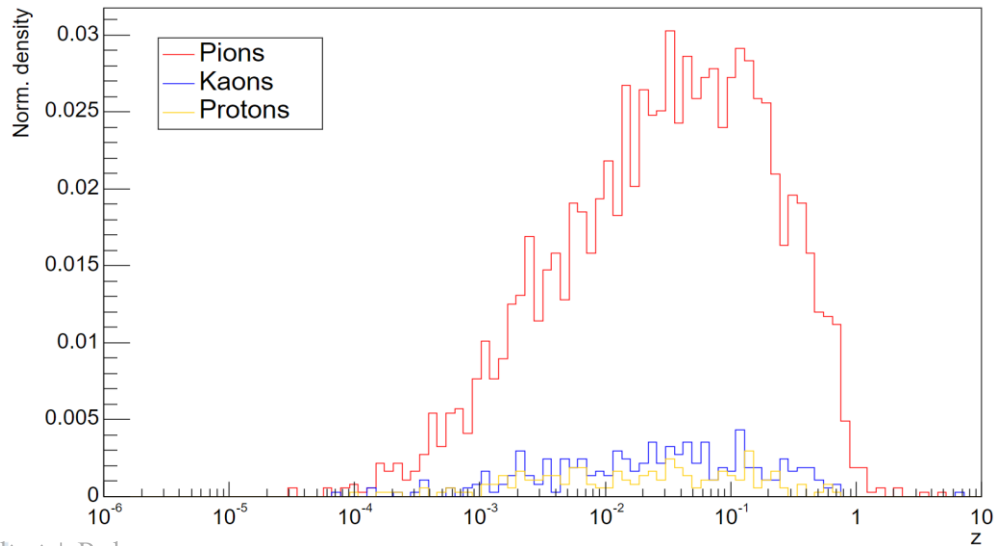


NORM. COUNTS vs z | NEGATIVE CASE

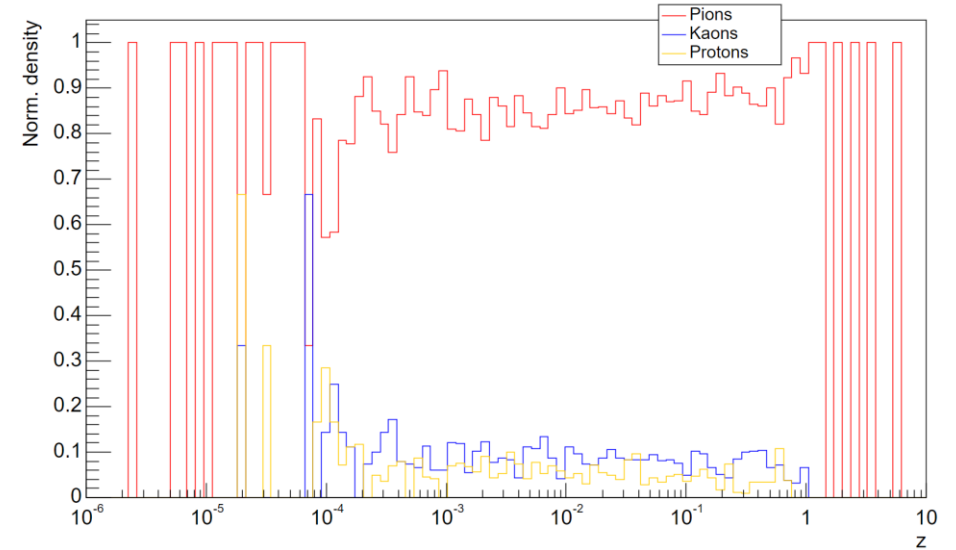
MC Production of negative particles | 18x275 GeV



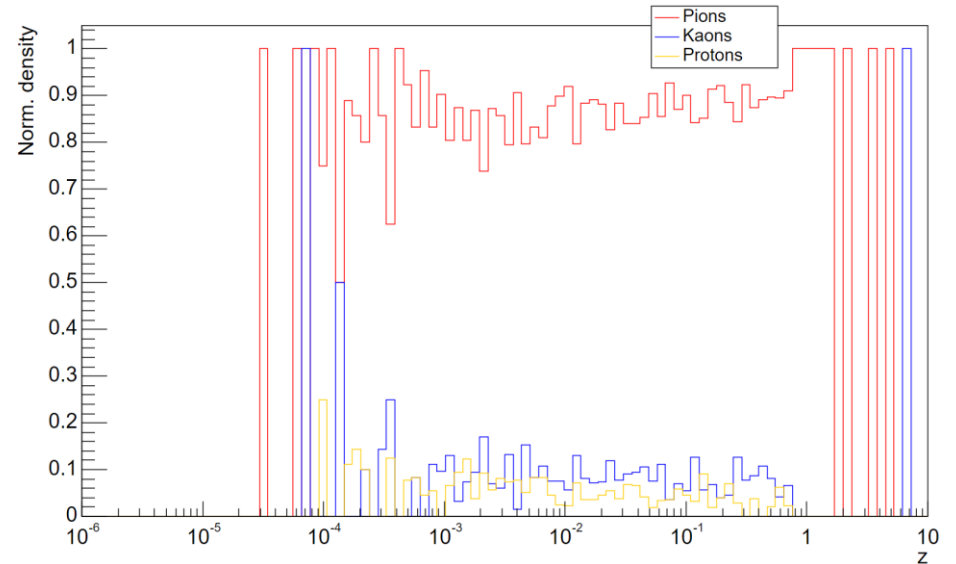
Reconstruction of negative particles | 18x275 GeV



MC Production of negative particles | 18x275 GeV

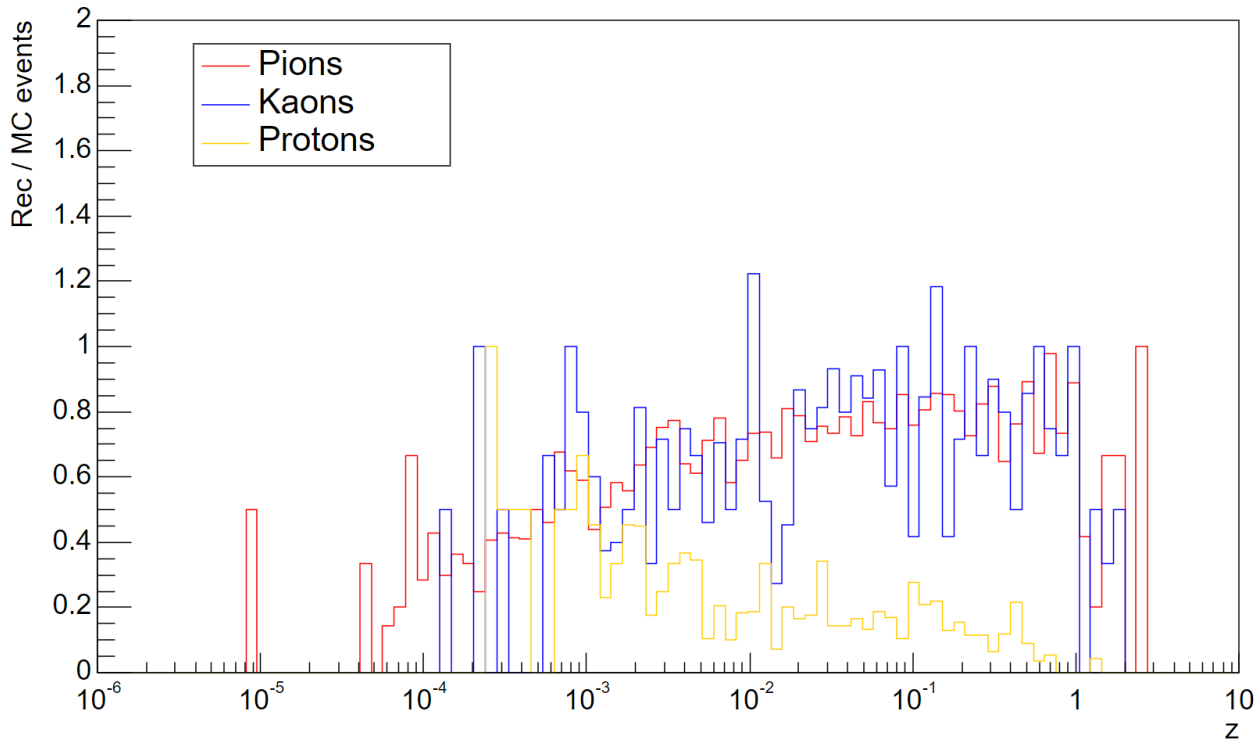


Reconstruction of negative particles | 18x275 GeV

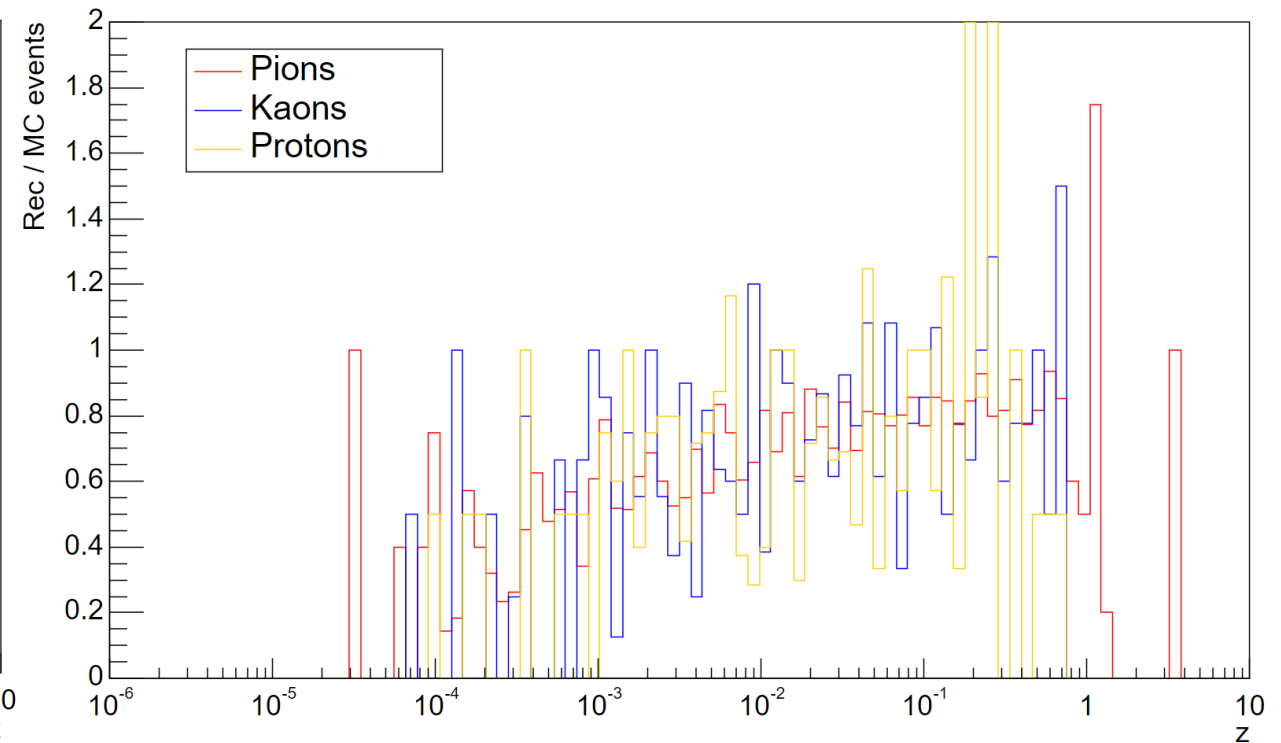


EFFICIENCY VS z

Efficiency reconstruction of positive particles | 18x275 GeV



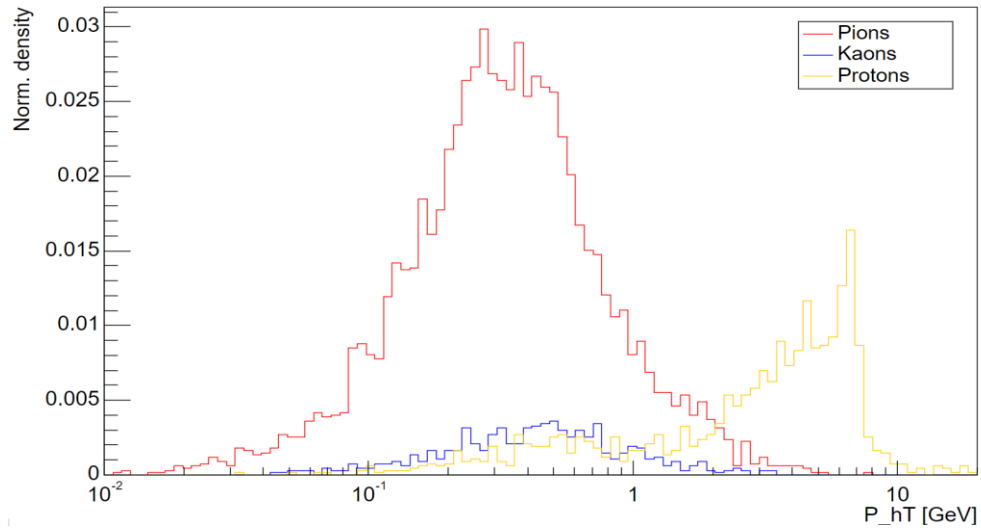
Efficiency reconstruction of negative particles | 18x275 GeV



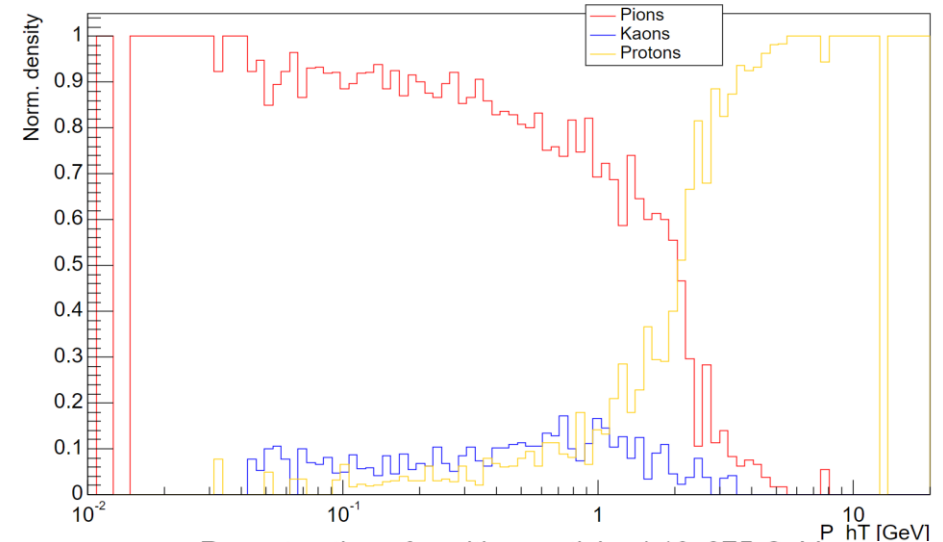
NORM. COUNTS vs P_{hT}

POSITIVE CASE

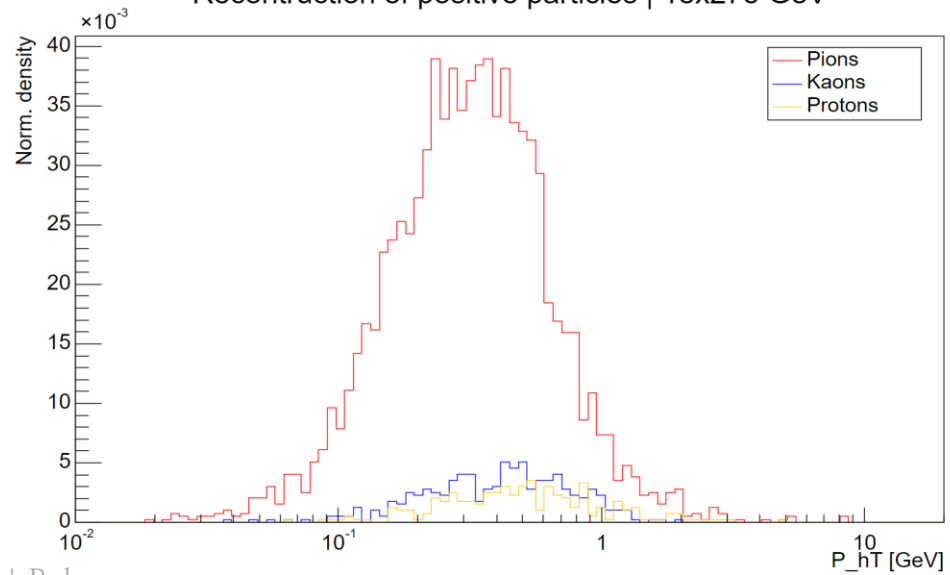
MC Production of positive particles | 18x275 GeV



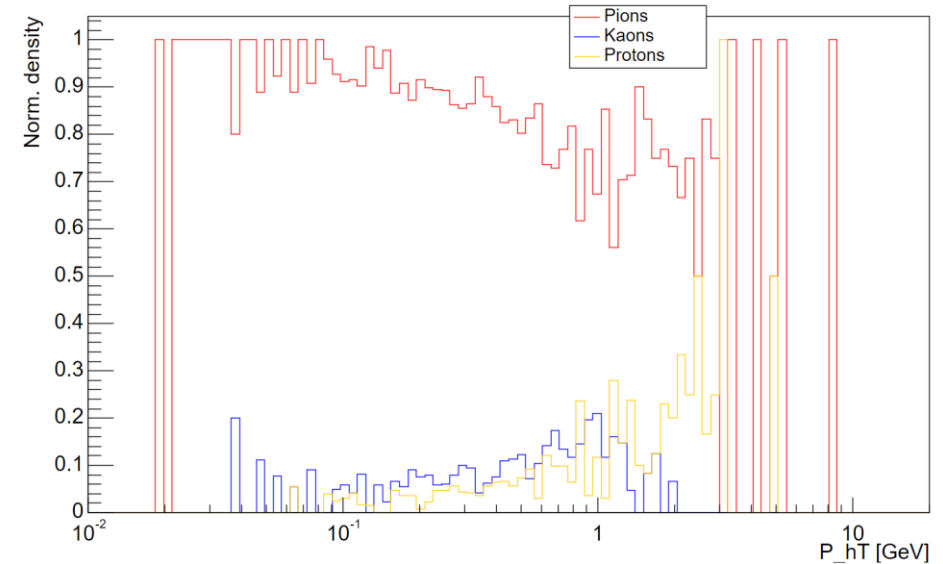
MC Production of positive particles | 18x275 GeV



Reconstruction of positive particles | 18x275 GeV



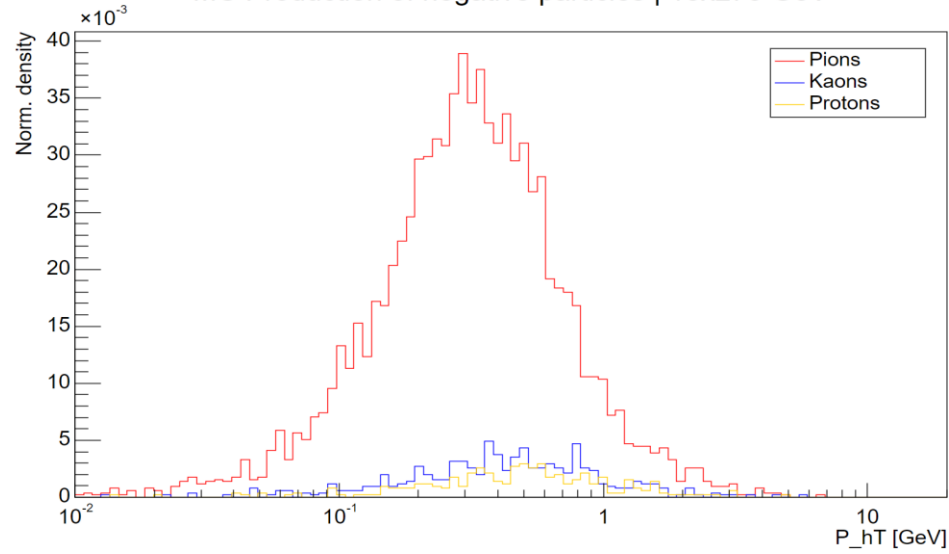
Reconstruction of positive particles | 18x275 GeV



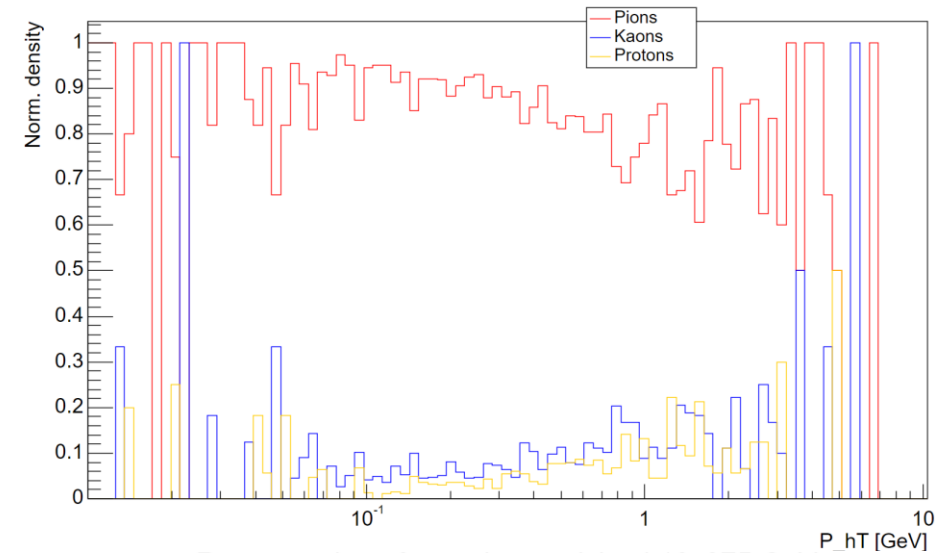
NORM. COUNTS vs P_{hT}

NEGATIVE CASE

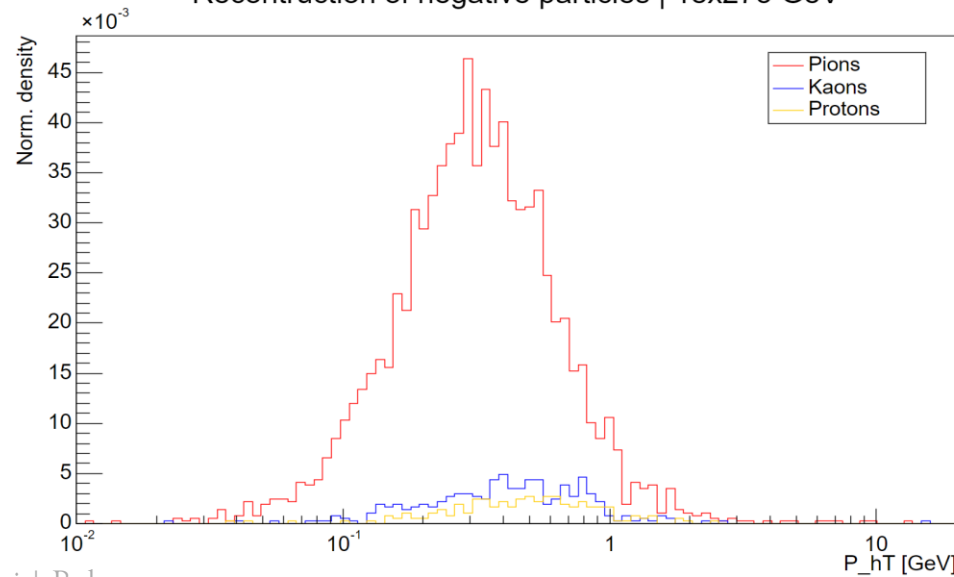
MC Production of negative particles | 18x275 GeV



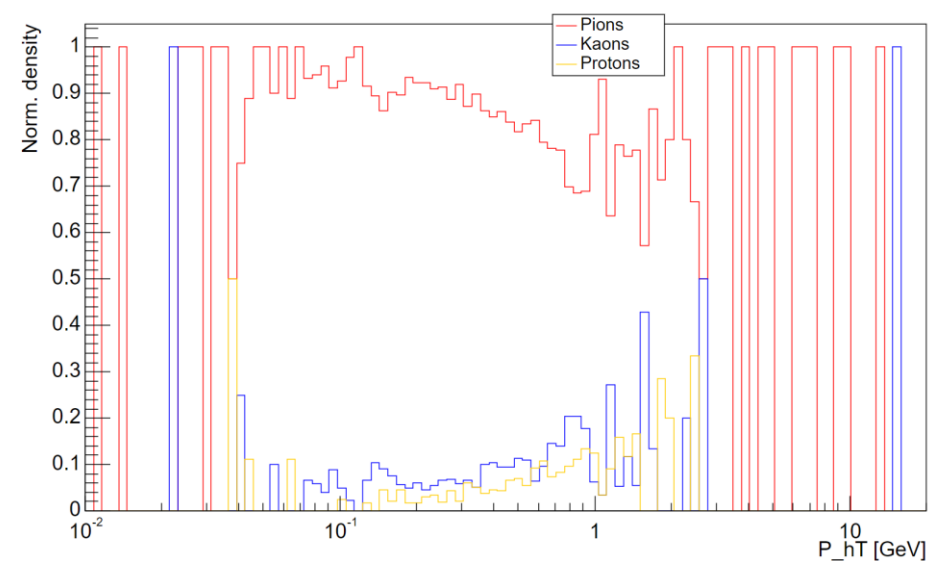
MC Production of negative particles | 18x275 GeV



Reconstruction of negative particles | 18x275 GeV

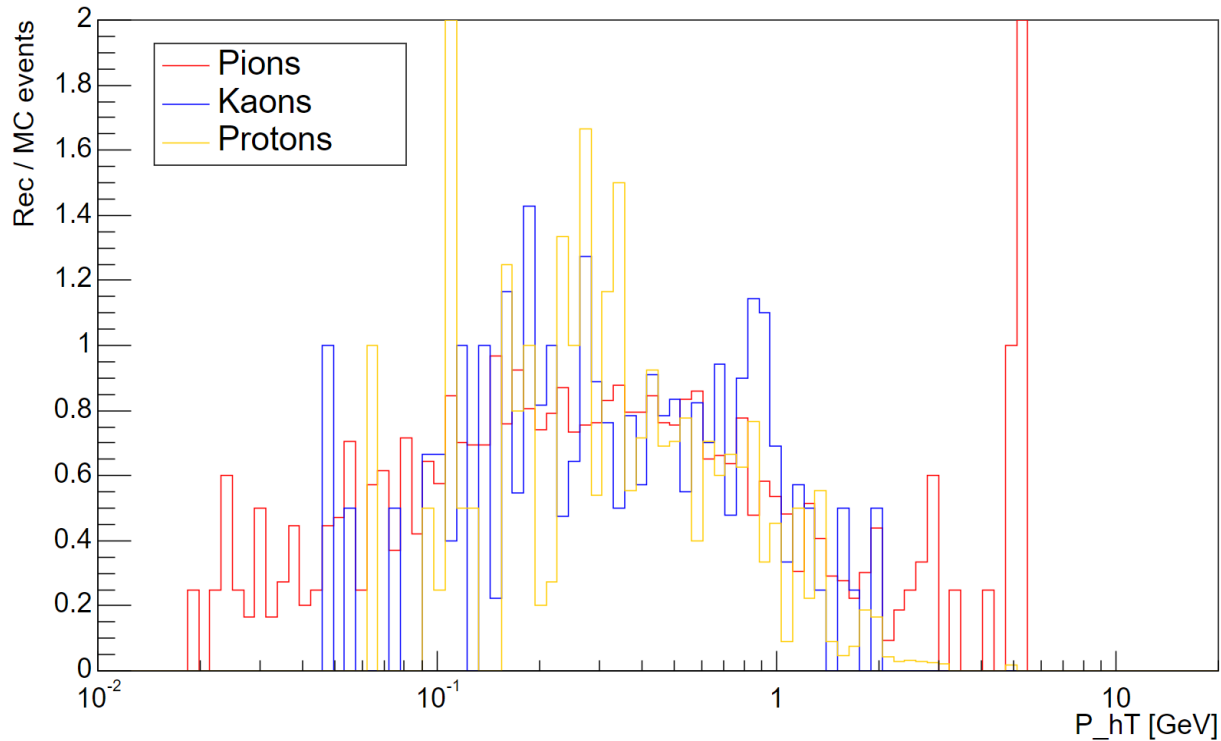


Reconstruction of negative particles | 18x275 GeV

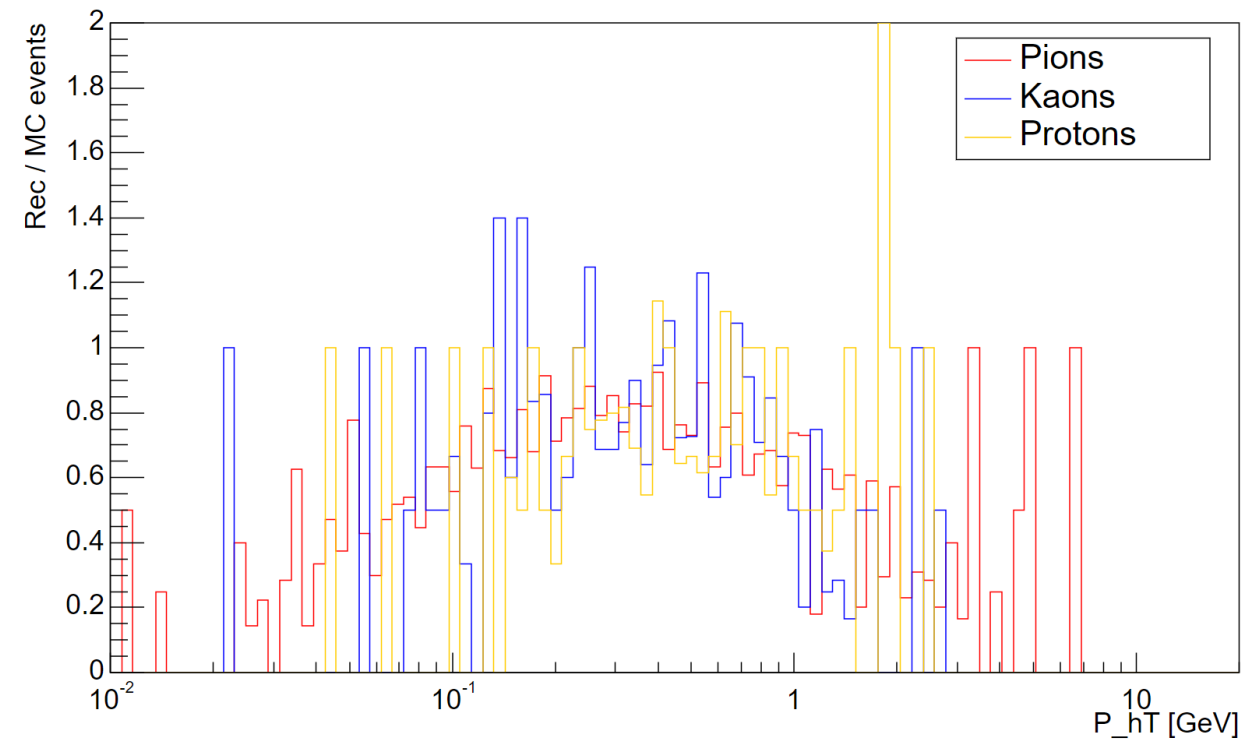


EFFICIENCY VS P_{hT}

Efficiency reconstruction of positive particles | 18x275 GeV

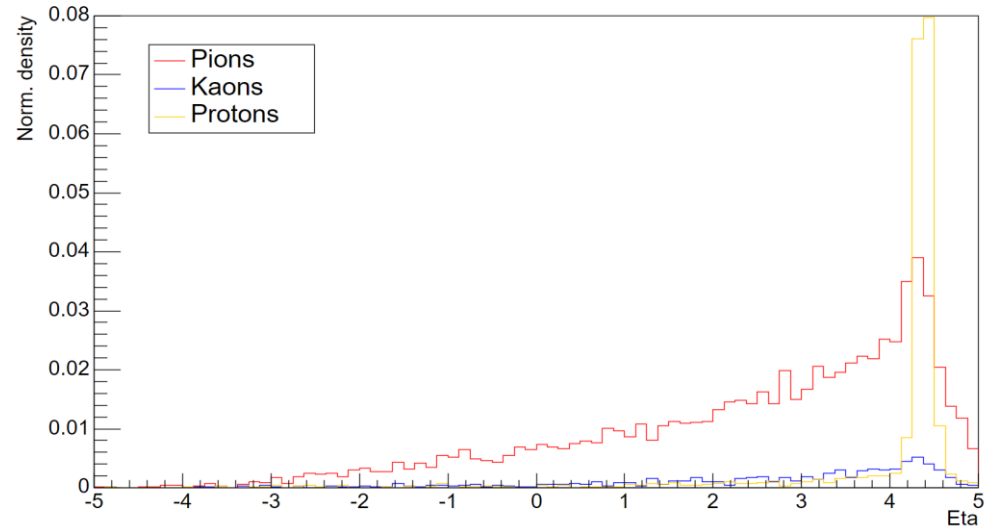


Efficiency reconstruction of negative particles | 18x275 GeV

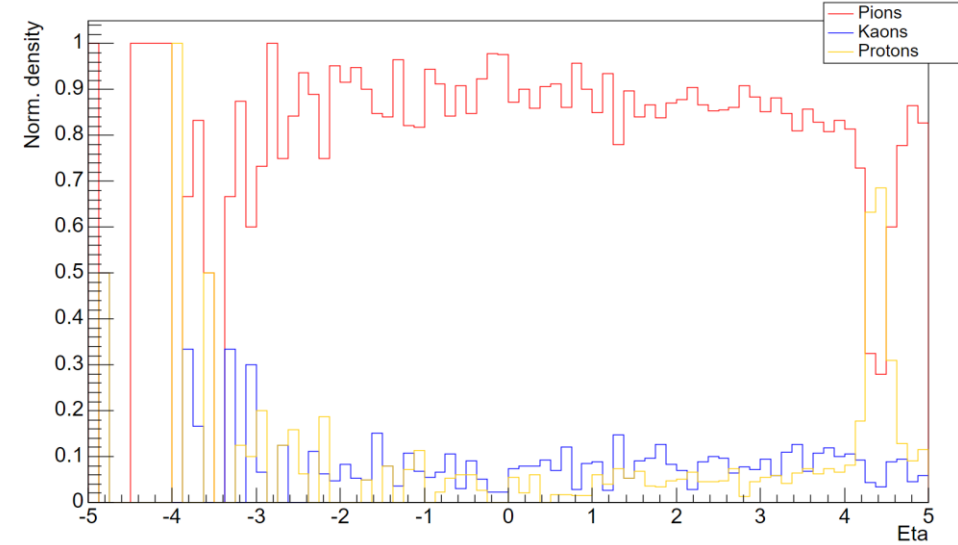


NORM. COUNTS vs η | POSITIVE CASE

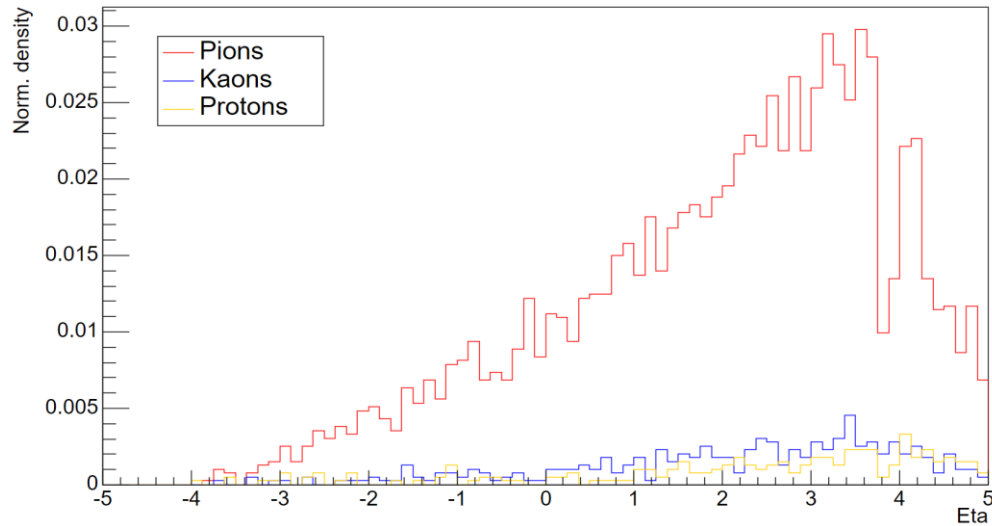
MC Production of positive particles | 18x275 GeV



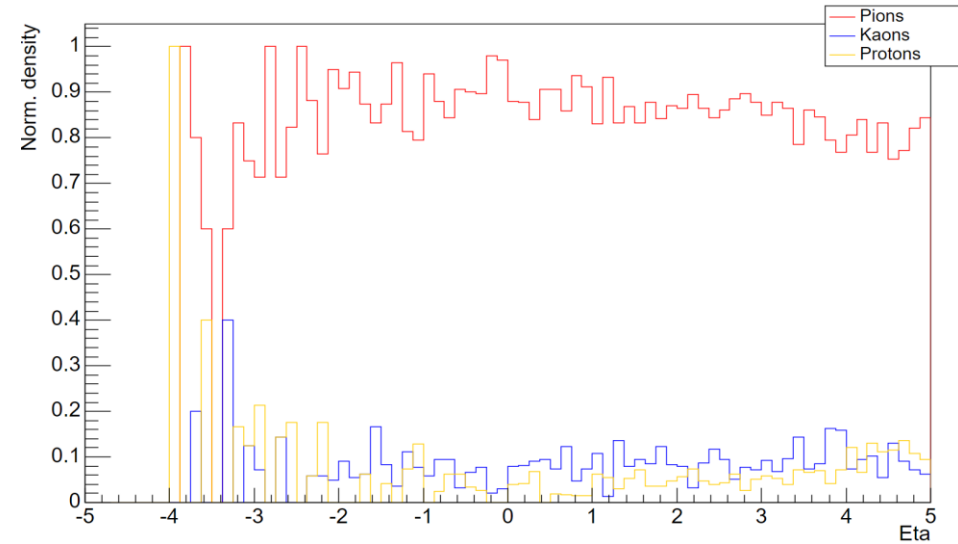
MC Production of positive particles | 18x275 GeV



Reconstruction of positive particles | 18x275 GeV

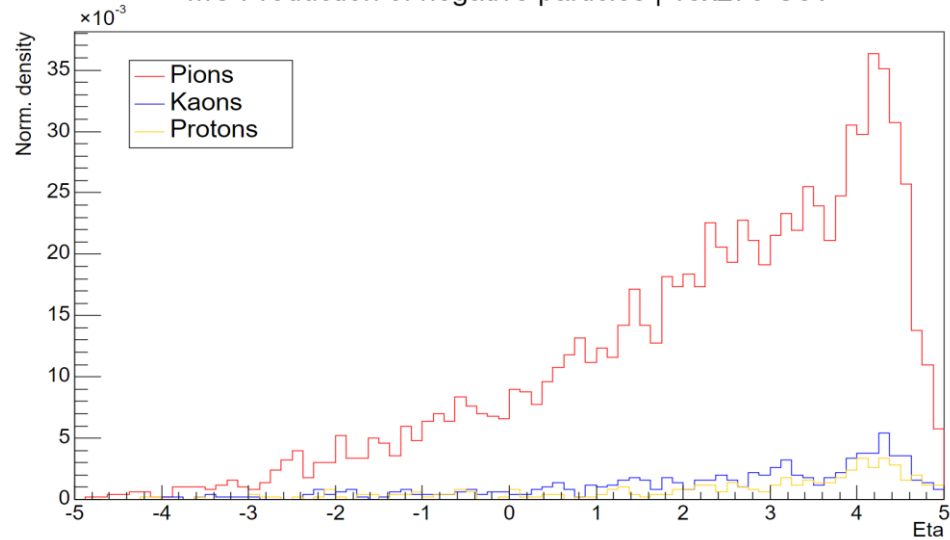


Reconstruction of positive particles | 18x275 GeV

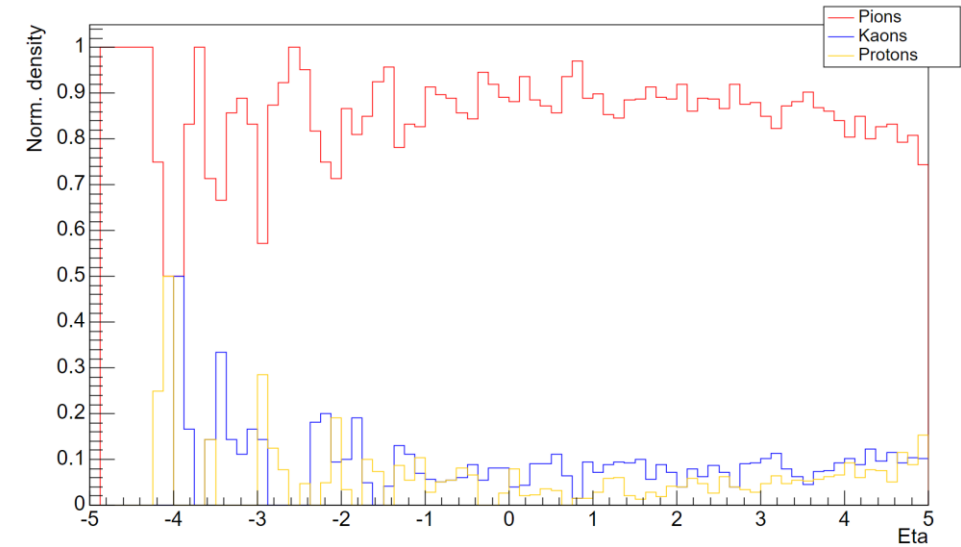


NORM. COUNTS vs η | NEGATIVE CASE

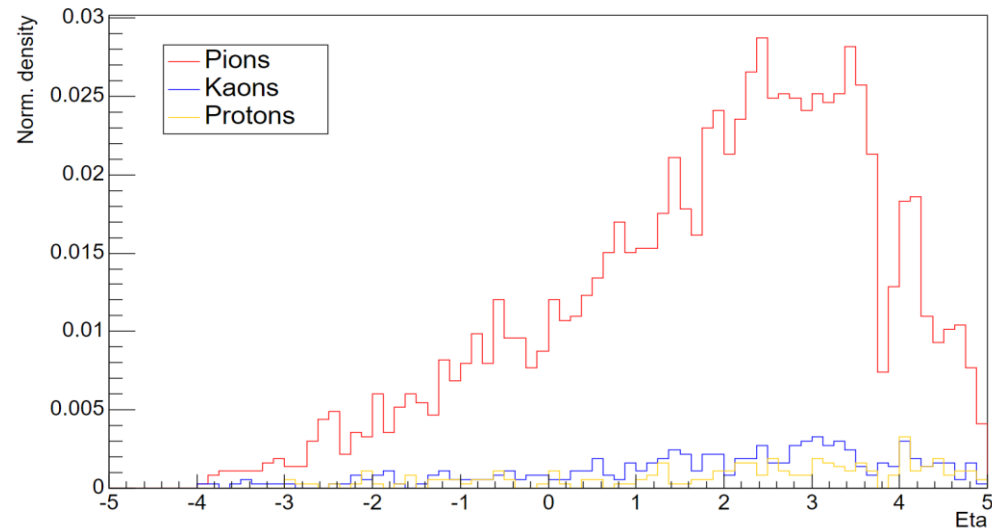
MC Production of negative particles | 18x275 GeV



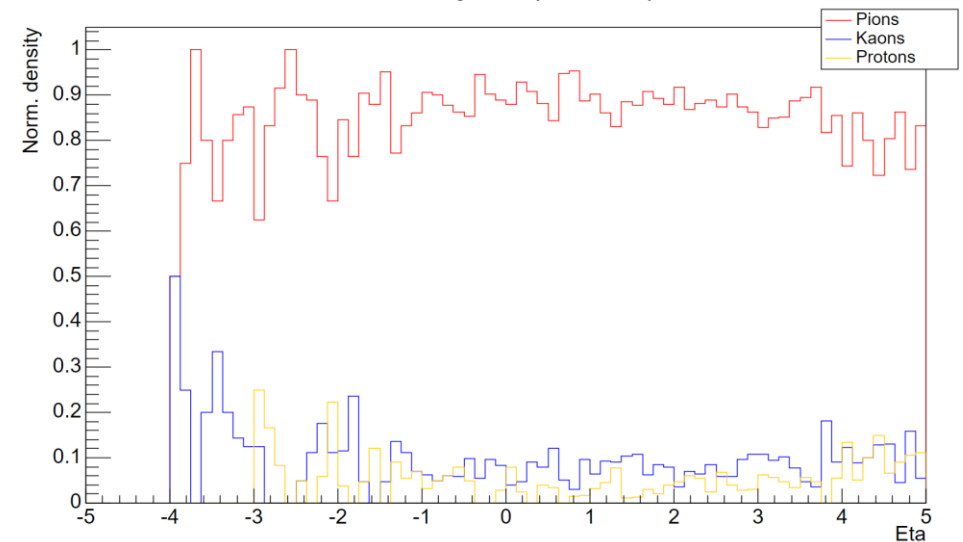
MC Production of negative particles | 18x275 GeV



Reconstruction of negative particles | 18x275 GeV

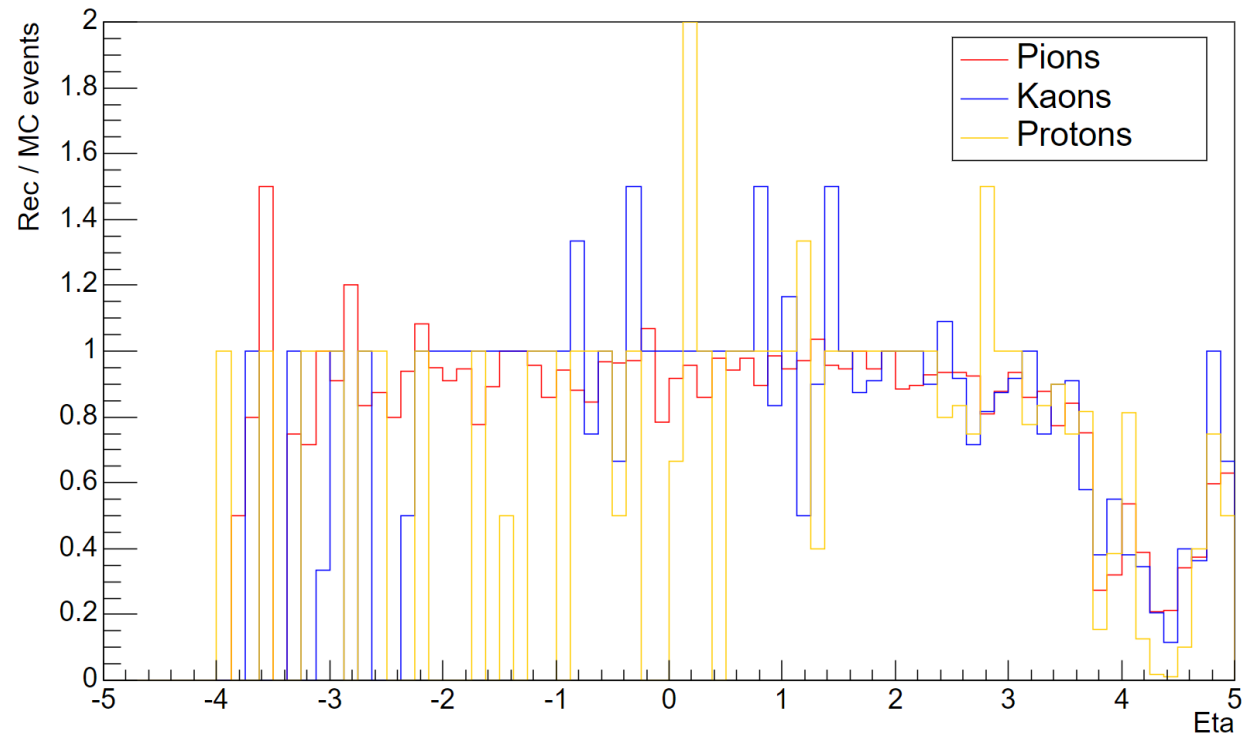


Reconstruction of negative particles | 18x275 GeV

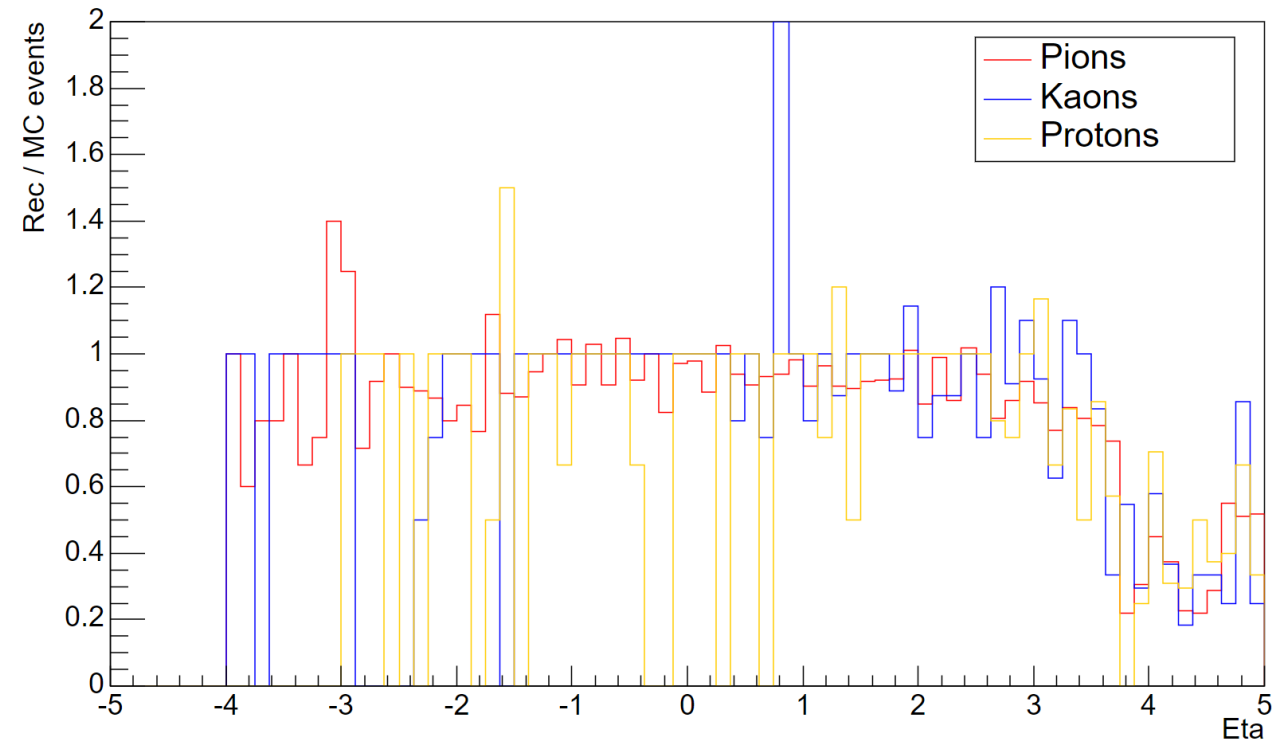


EFFICIENCY VS η

Efficiency reconstruction of positive particles | 18x275 GeV



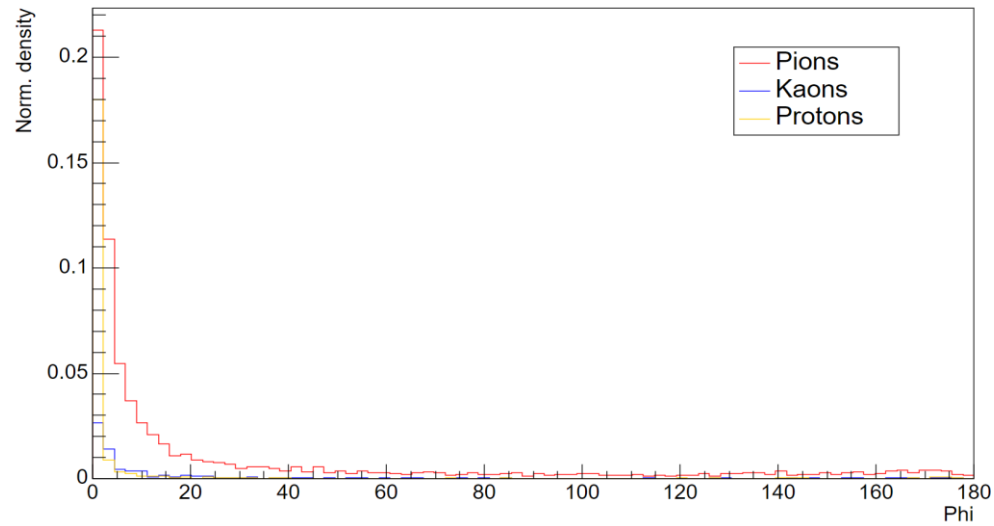
Efficiency reconstruction of negative particles | 18x275 GeV



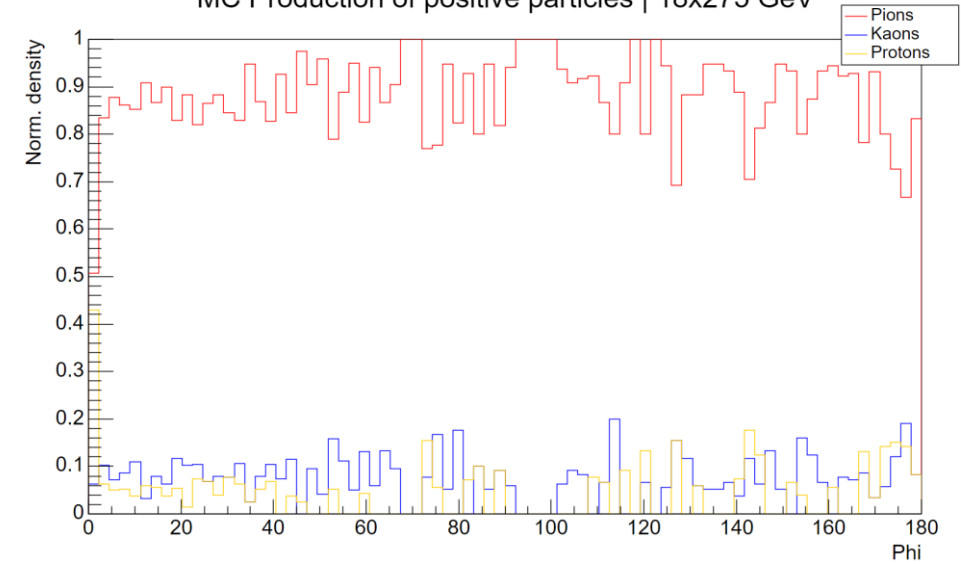
No cuts were performed in the pseudorapidity.

NORM. COUNTS vs φ | POSITIVE CASE

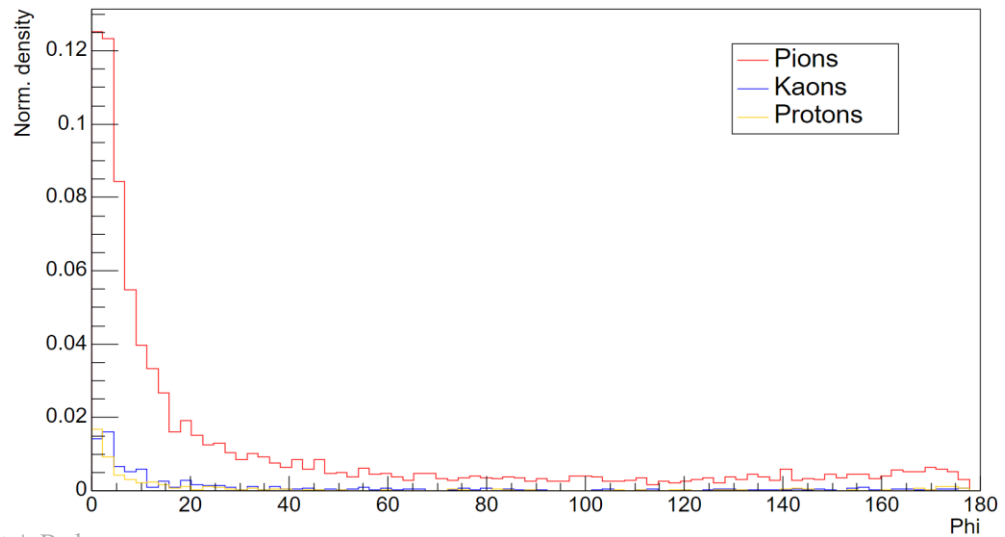
MC Production of positive particles | 18x275 GeV



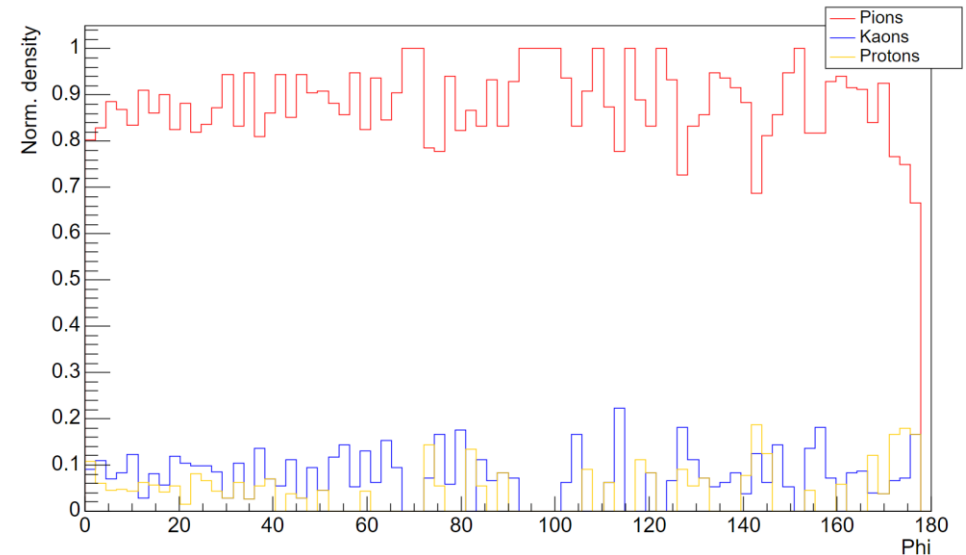
MC Production of positive particles | 18x275 GeV



Reconstruction of positive particles | 18x275 GeV

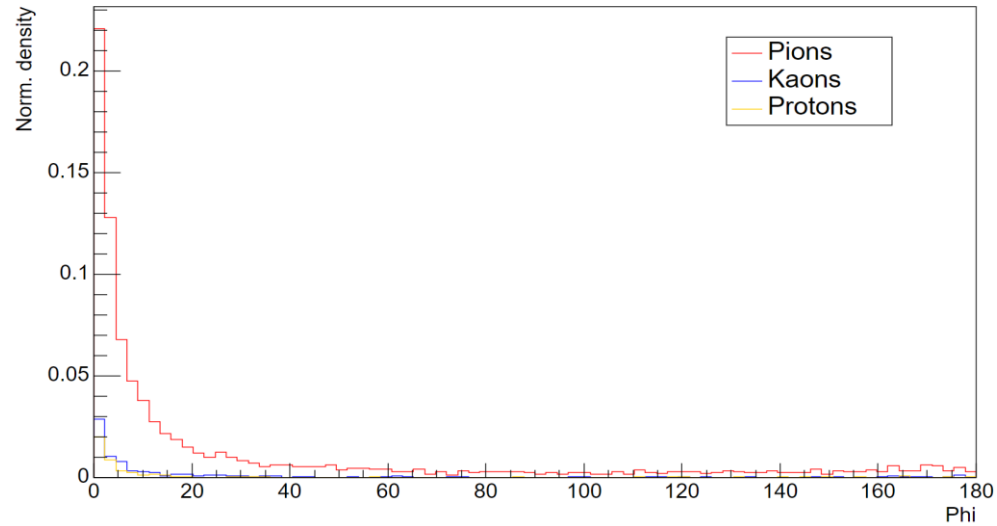


Reconstruction of positive particles | 18x275 GeV

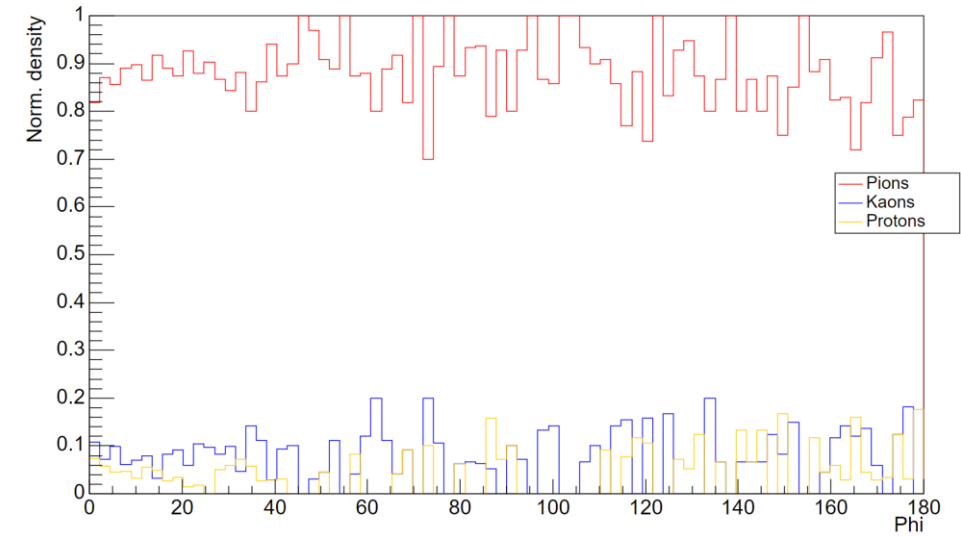


NORM. COUNTS vs φ | NEGATIVE CASE

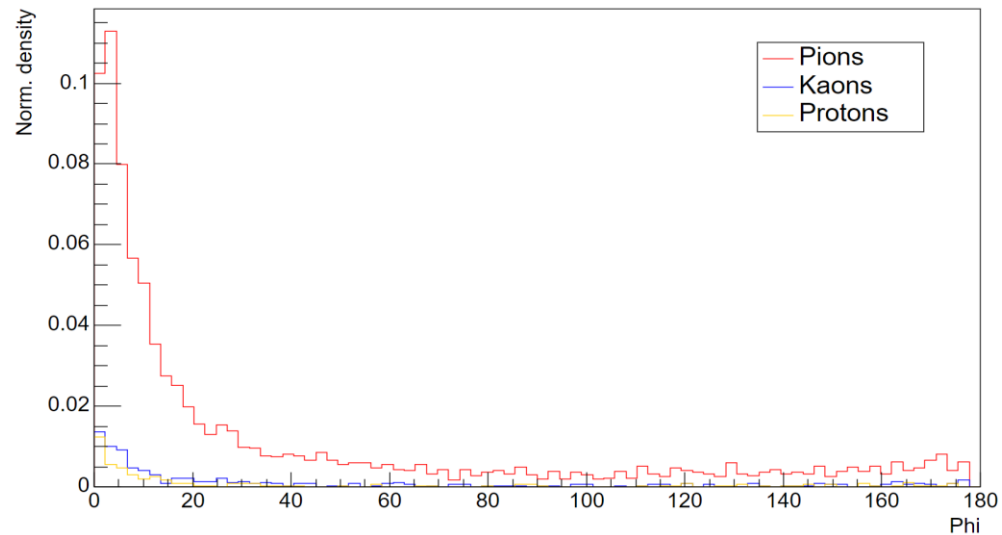
MC Production of negative particles | 18x275 GeV



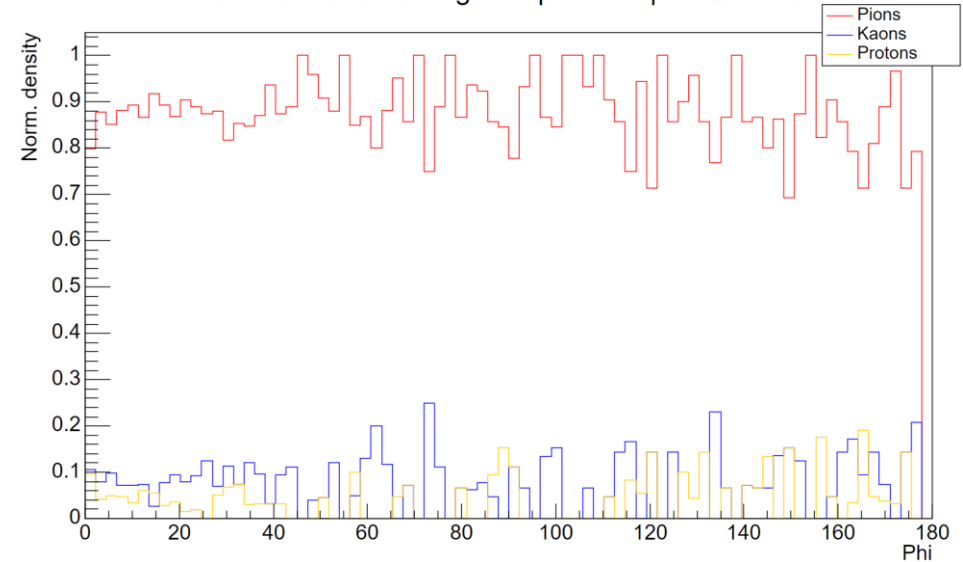
MC Production of negative particles | 18x275 GeV



Reconstruction of negative particles | 18x275 GeV

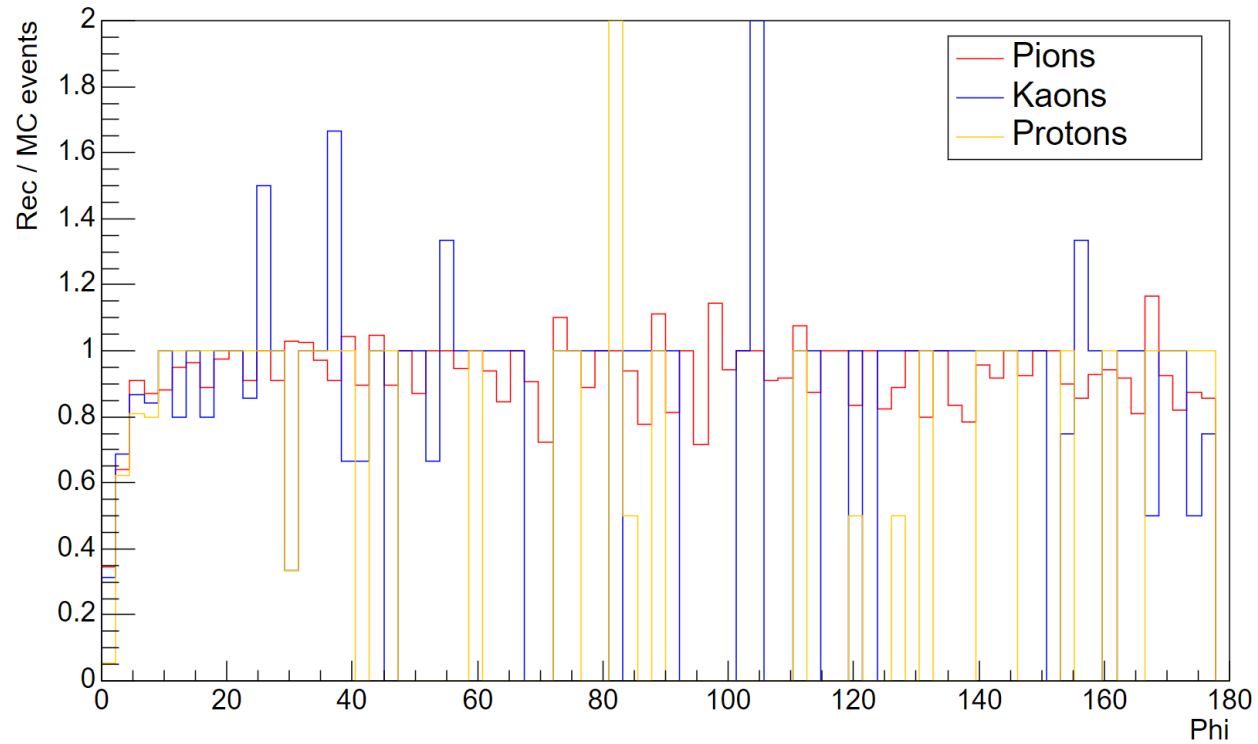


Reconstruction of negative particles | 18x275 GeV

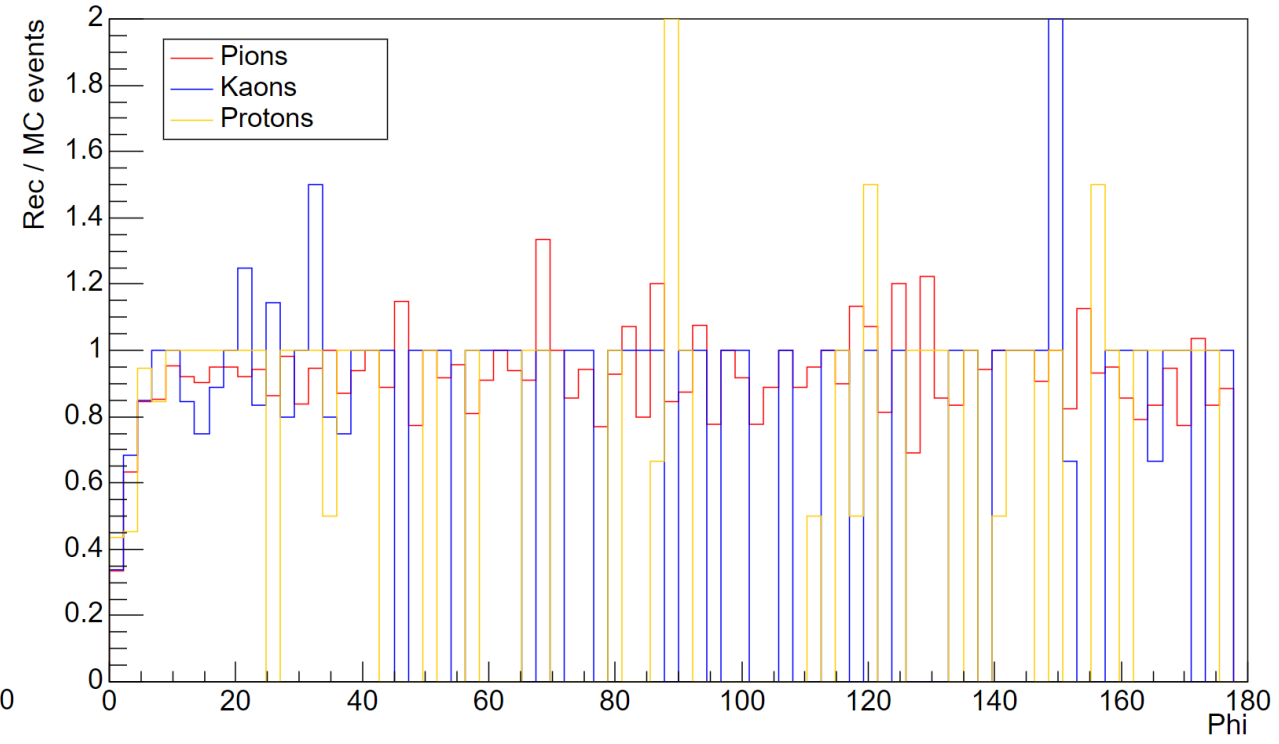


EFFICIENCY VS φ

Efficiency reconstruction of positive particles | 18x275 GeV

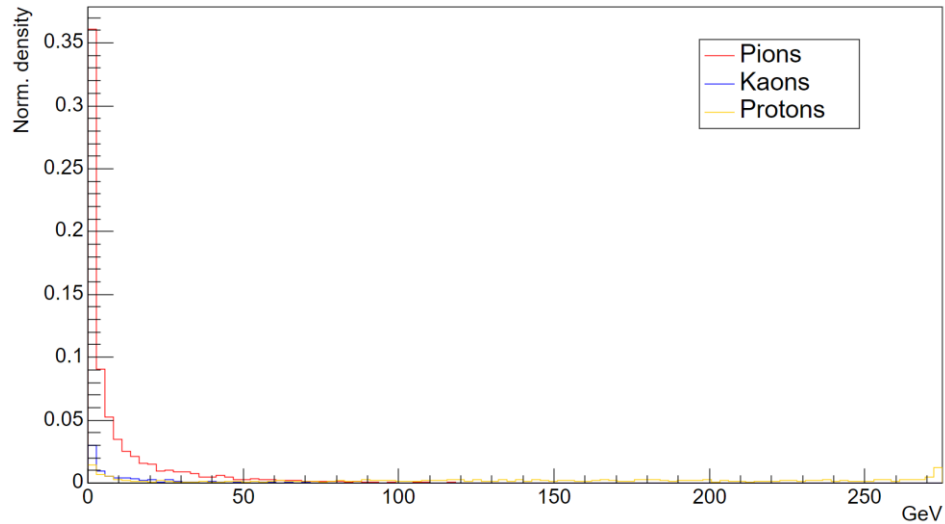


Efficiency reconstruction of negative particles | 18x275 GeV

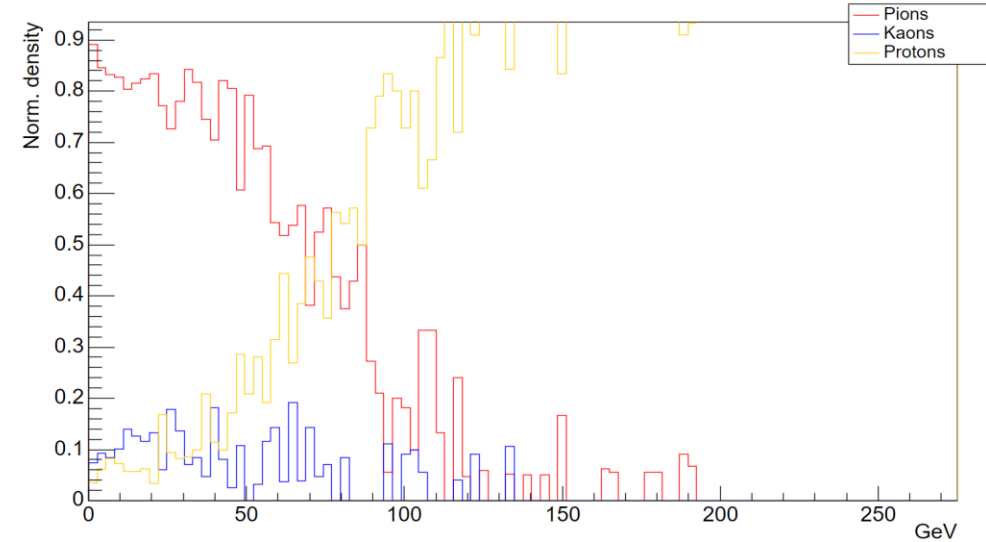


NORM. COUNTS vs *mom* | POSITIVE CASE

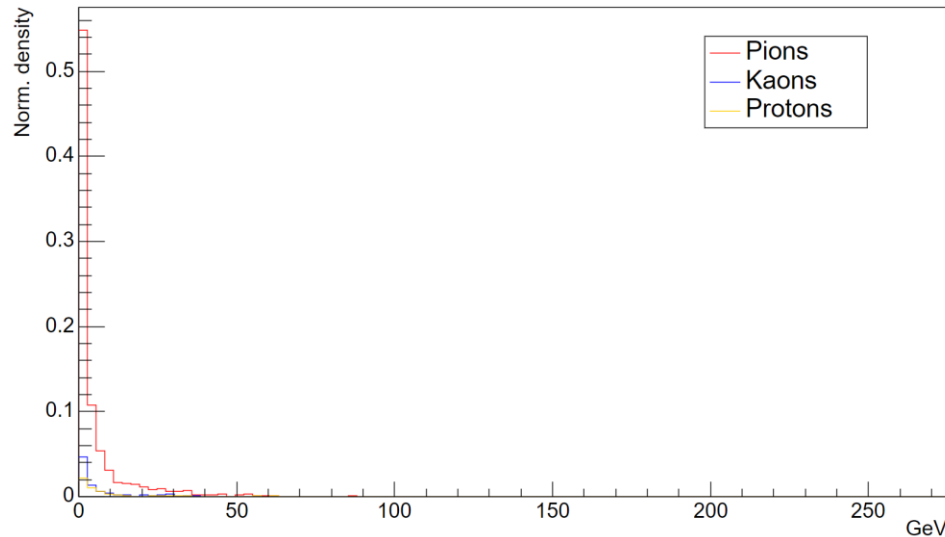
Production of positive particles with the Momentum



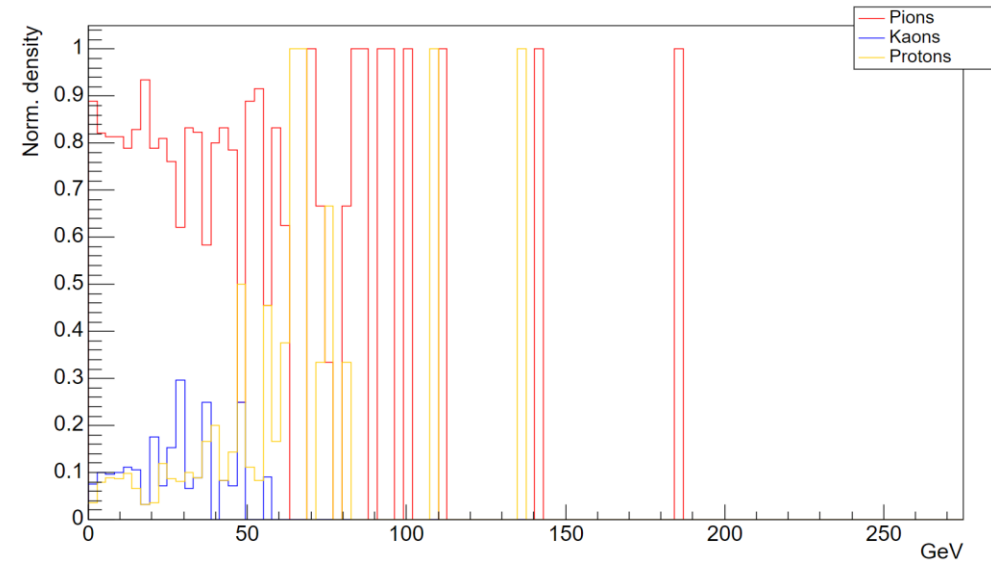
Production of positive particles with the Momentum



Production of positive particles with the Momentum



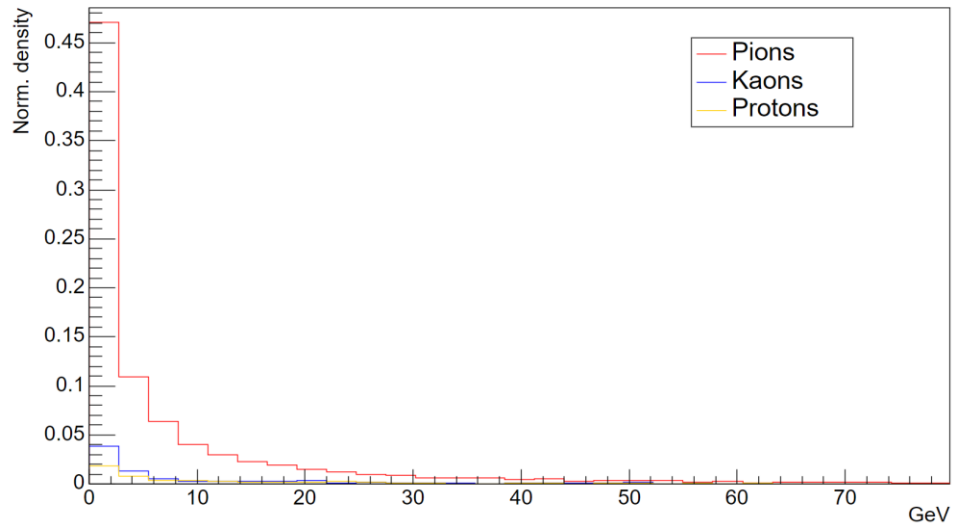
Production of positive particles with the Momentum



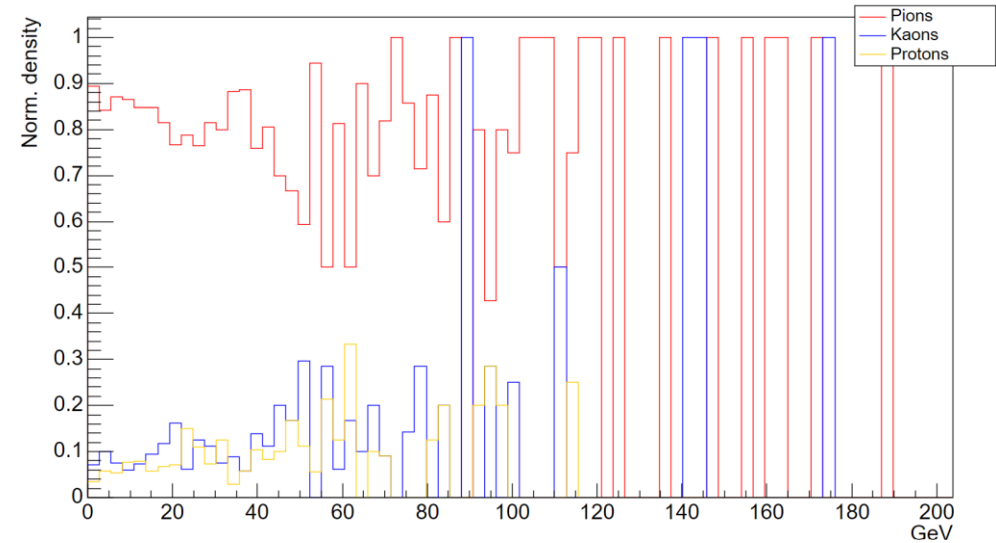
NORM. COUNTS vs *mom*

NEGATIVE CASE

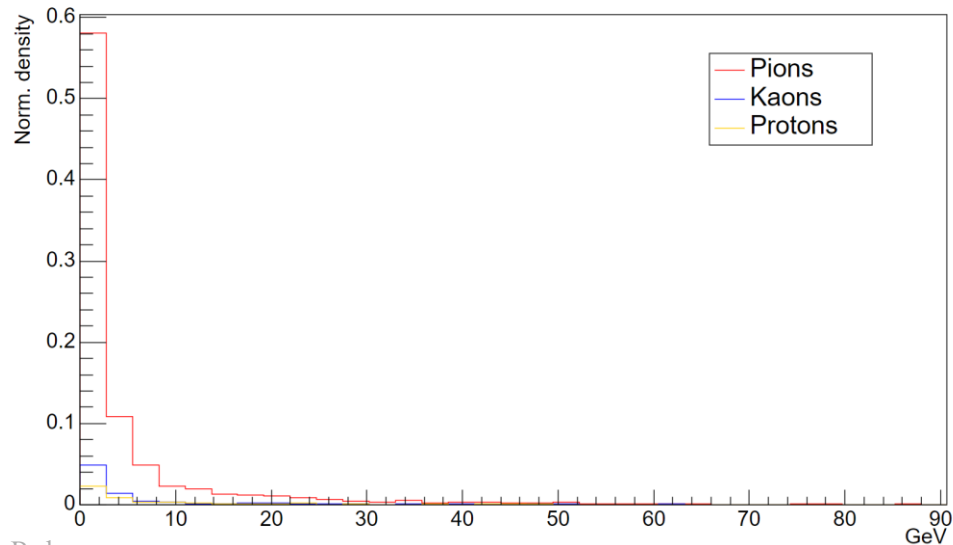
Production of negative particles with the Momentum



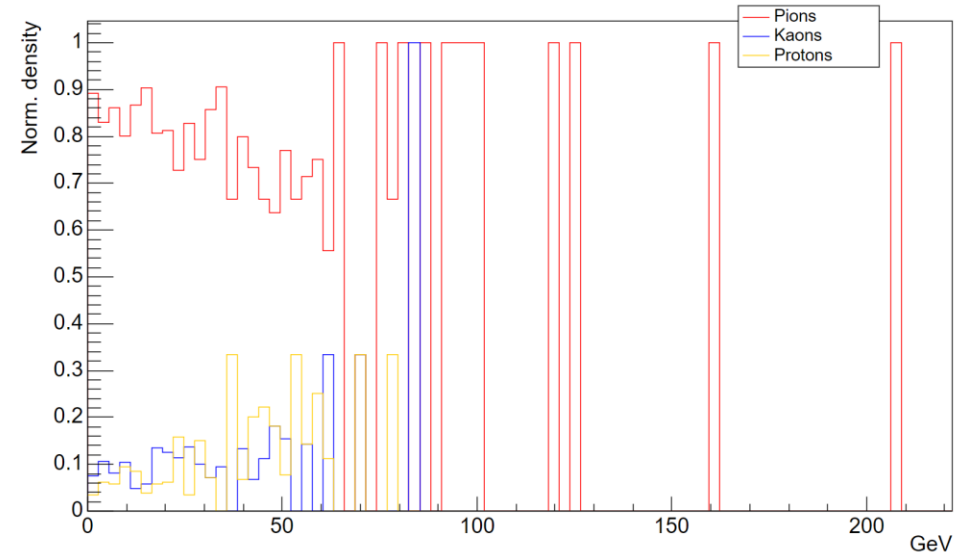
Production of negative particles with the Momentum



Production of negative particles with the Momentum

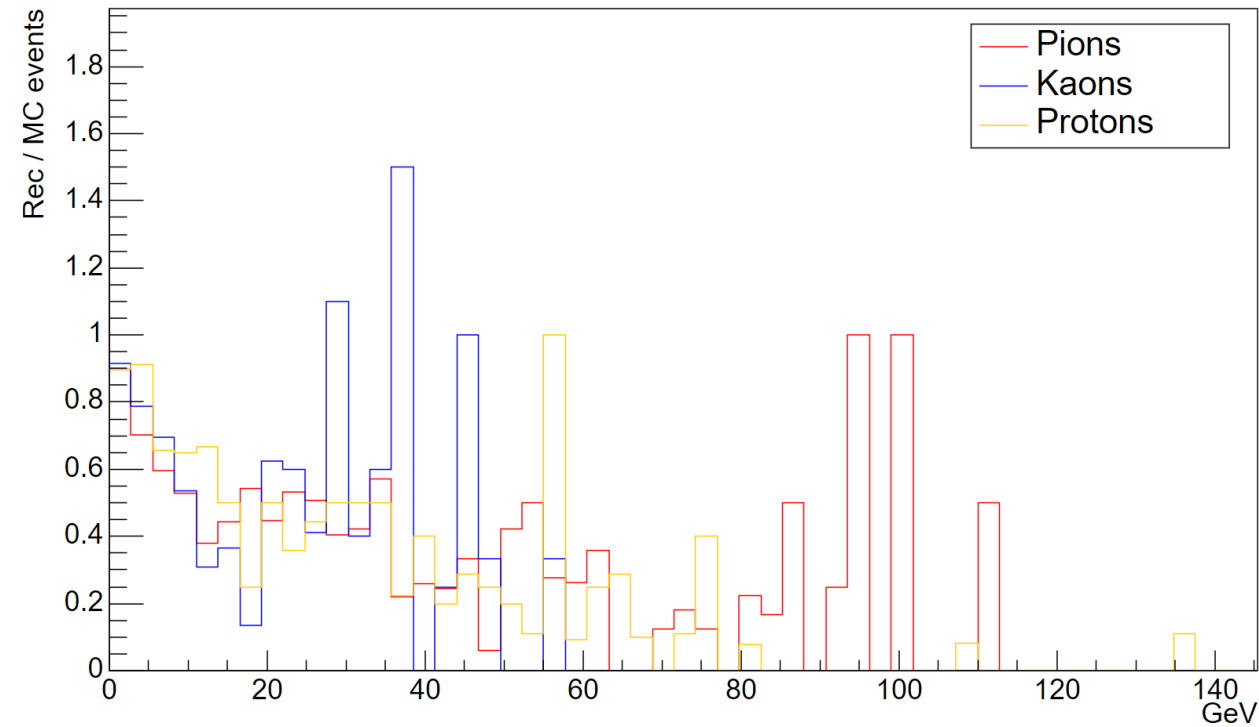


Production of negative particles with the Momentum

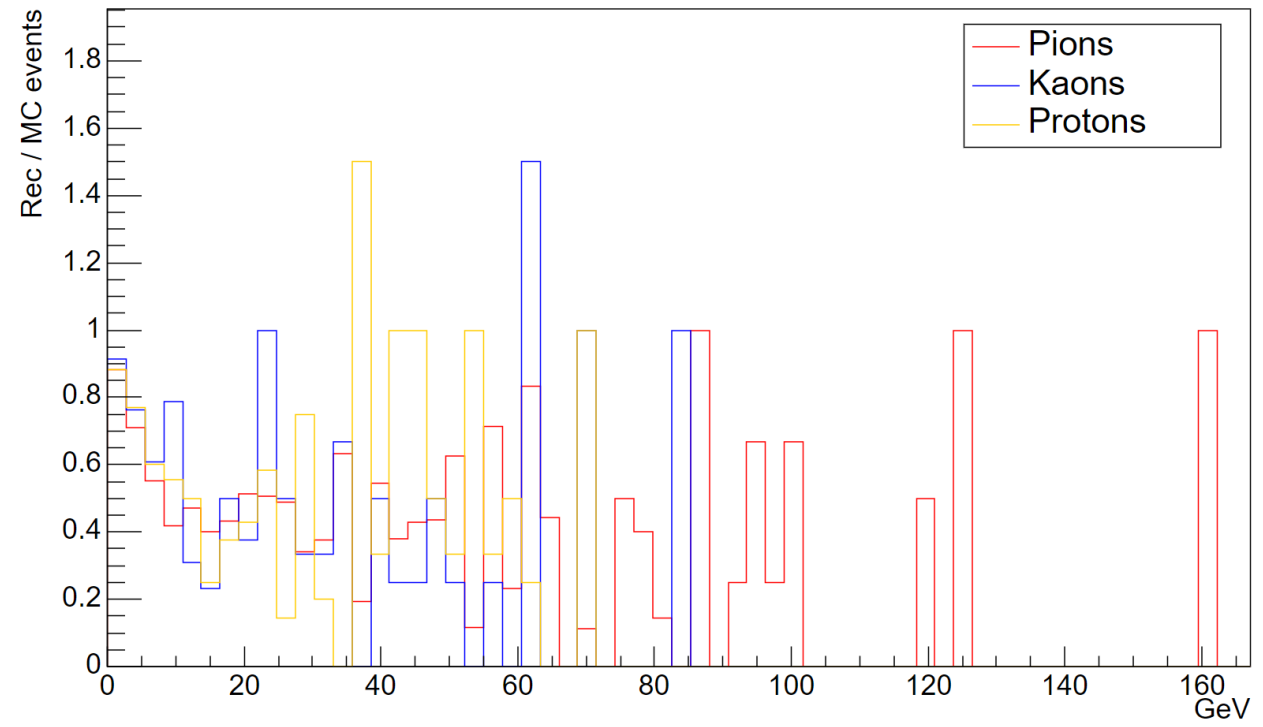


EFFICIENCY VS *mom*

Efficiency reconstruction of positive particles | 18x275 GeV



Efficiency reconstruction of negative particles | 18x275 GeV



More statistic and the integration of region cuts are needed.

SUMMARY

The calculations were made over a small fraction of the data, as shown in the first slide, due to personal technical limitation. The opportunity to use more data would enhance the performance of the current simulations.

Nevertheless, the current PID technique shows the low ability in reconstructing these hadrons across particular kinematic ranges. Future integrations in the simulated data are necessary to improve the reconstruction performances and gain a better understanding of the physics at the EIC.

THANKS FOR YOUR ATTENTION